Sediment yield by gully erosion in a sub catchment of the Awassa watershed, Ethiopia

- MSc thesis -

Universiteit Utrecht

P.E. Hoogenboom
January 2013

Sediment yield by gully erosion in a sub catchment of the Awassa watershed, Ethiopia

- MSc thesis -

MSc Thesis Physical Geography
P.E. Hoogenboom

Faculty of Geosciences
Department of Physical Geography
Utrecht University

Under supervision of
Prof. S.M. de Jong
Dr. G. Sterk

January 2013

Universiteit Utrecht

Abstract

Lake Awassa is a lake in the Ethiopian Rift Valley and undergoes a water level rise since the last few decades. Local people say that this increase is caused by an increase in surface runoff due to deforestation. Another hypothesis suggests that the water level rise is due to siltation of the lake by erosion and especially gully erosion. To investigate the second hypothesis, a sub catchment of the Awassa watershed is observed in detail. In this area gully erosion is observed in 2012 by carrying out a field survey and in 1972 by stereo aerial photography. The sub catchment consists of two gully systems which contain 12 gullies in total. Gully dimension measurements were done in the field and with the aerial photographs to obtain the gully erosion rate over the last 40 years. In addition the land use was classified in 1986, 1994 and 2011 by Landsat 5 TM imagery to link the gully erosion with land use changes. After processing all the data, accurate gully measurements with the aerial photographs turned out to be impossible due to poor quality of the digitized photos. The volumes and gully erosion rates were calculated, assuming that the gullies started developing in 1972. The total volume of gully system 1 is 965000 m^3 and the gully erosion rate is 23.4 t $ha^{-1}y^{-1}$, for gully system 2 the total volume is estimated to be 1778000 m^3 and the gully erosion rate 20.7 t $ha^{-1}y^{-1}$. Both gully systems are active and observations in the field indicate that gully system 2 is connected with Lake Awassa and deposits its sediment in the lake. There can be concluded that gully erosion contributes to siltation of Lake Awassa.

Contents

1. Introduction

Land degradation is any undesirable or damaging change or disturbance of the land and decreases the productive capacity of the land. Land degradation is a well known problem in Ethiopia, causing severe food shortages and famine (Taddese 2001). The major sources of food and incomes like agricultural land, pastures, forests and woodlands are degraded for 30% (Sheikh et al. 2006). Land degradation is at global scale mainly caused by erosion of the fertile soil (Tesfahunegn et al. 2012). Erosion of the soil can occur due to natural factors like wind and water, human impact or a combination of both. Most of the soil loss in Ethiopia occurs on crop land and unproductive land, respectively 42 and 70 t $ha^{-1}y^{-1}$ (Hurni 1987). This research focuses on gully erosion, a form of soil erosion caused by water that in some cases is triggered by human activity. Gully erosion can occur in the form of ephemeral gullies, permanent or classical gullies or bank gullies and contributes significantly to the amount of soil loss in an area.

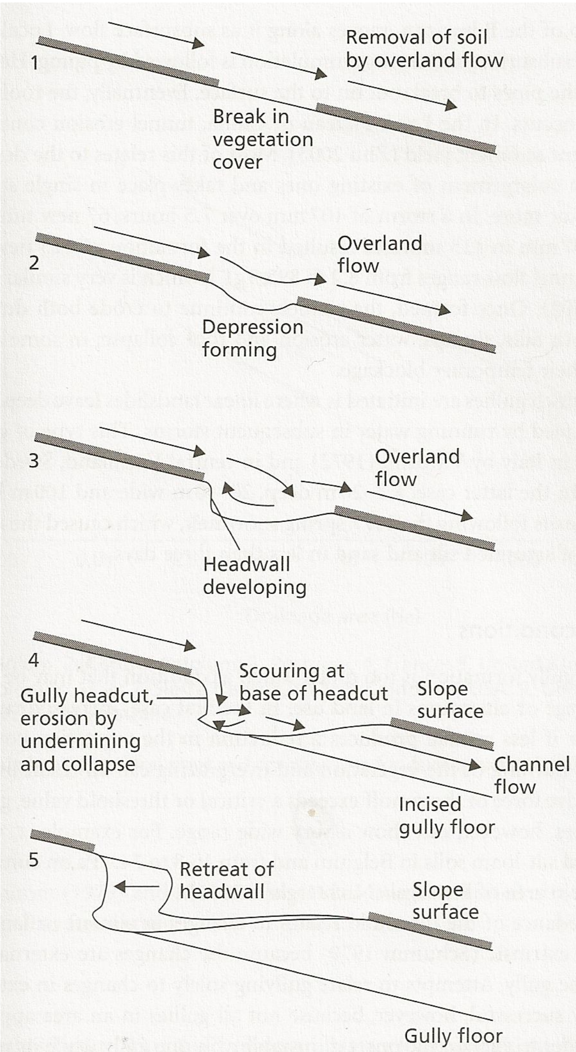

Fig. 1.1. Stages in the surface development of gullies on a hillside (after Leopold et al. 1964).

Figure 1.1 shows the stages in the surface development of gullies on a hillside. Gully erosion is defined as the erosion process whereby runoff water accumulates and often recurs in narrow channels and, over short periods, removes the soil from this narrow area to considerable depths (Poesen et al. 2003). The runoff in a gully transports sediment from upland to the valley into permanent channels and increases there the effects of water erosion (Valentin et al. 2005). An ephemeral gully is a form of gully erosion that in size lies between rill erosion and the classical gully erosion. The term ephemeral gully was introduced in the 1980's to include a sediment source that was, until that time overlooked in the traditional soil erosion assessments (Foster 1986, Grissinger 1996a,b). The definition for ephemeral gullies by the Soil Science Society of America (2001) is as follows, they are small channels eroded by concentrated overland flow that can easily be filled by normal tillage and they will only reform again in the same location by additional runoff events. Different criteria are used to distinguish ephemeral gullies from rills. Poesen (1993) used the criteria of a critical cross-sectional area of 929 cm^2 (square foot criterion), first used by Hauge (1977). Other criteria's are a minimum width of 0.3 m and a minimum depth of about 0.6 m (Brice 1966) or 0.5 m (Imeson et al. 1980). A permanent or classical gully can not be removed, like an ephemeral gully could be, with ordinary farm tillage equipment. The depth of classical gullies range between a depth of 0.5 m to as much as 25-30 m. Bank gullies are formed due to a height drop caused by a terrace or a river bank. The soil loss due to gully erosion is depended on the types of gully erosion present in an area. For each type of gully erosion the amount of soil loss varies from region to region, caused by differences in soil type. Other factors affecting the amount of soil loss by gully erosion are the spatial and temporal scale, land use, climate and weather conditions and the topography. Thereby, the process of gully erosion is clearly dependent on a variety of thresholds. Gully erosion only occurs when a certain threshold has been exceeded, a few of them are flow hydraulics, rainfall, topography, pedology and land use (Poesen et al. 2003).

Gully erosion can have a great impact on for instance agricultural land and infrastructures. Fertile soils from upstream are eroded and deposited at the end of the gully, making the upstream area infertile and unusable for agriculture. When the erosion continuous and gullies form, infertile soils are eroded from out of the gullies and deposited at the end of the gullies. Due to this the sedimentation areas of the gullies are unusable for agriculture. Contribution of gully erosion to the overall soil loss in the northern highlands of Ethiopia was measured to be 33 to 55%, which equals 4.7-12.1 t $ha^{-1}y^{-1}$ (Nyssen 2001). In this area different measures are taken to decrease the amount of soil loss by gully erosion. As conservation measures check dams are placed in the gullies and stone bunds and exclosures are used in the intergully zones. The check dams are used to prevent the development of permanent gullies in rangeland and cropland (Nyssen et al. 2004a,b). However, not everywhere are these conservation measures adopted by farmers, even though they prove to be effective. Another research to gully erosion that is carried out is by Moges et al. (2008) in the Umbulo catchment in Southern Ethiopia. In this research the gully development in the Umbulo catchment is observed for 30 years, resulting in average soil loss rates from 11 to 30 t $ha^{-1}y^{-1}$. Besides their impact on agricultural land and infrastructure, gully erosion can also be an important source of sediments in reservoirs. The watershed of Lake Awassa in south central Ethiopia is an example of such an area where gully erosion is a problem. Around the lake, especially at the northwest side, great classical gully systems have developed. Land use changes over the past decades, when forest areas have been cleared and converted into agricultural land, may have resulted in increasing rates of gully erosion. The related amounts of sediment being transported from the gullies potentially end up in Awassa lake, where they are deposited, because the lake does not have an outlet (Ayenew et al. 2006; WWSDE 2001).

The level of lake Awassa has risen during the last 30 years (fig. 1.2). The figure shows an increasing trend of the water level and a cyclic fluctuation of about 5 years (Abiye 2008). The average water level rise is about 2 m in 34 years which is about 5.9 cm y^{-1}. The water level rise causes problems for the citizens of Awassa town and parts of the town are regularly flooded since the early 1970's (Ayenew 2007). Hence, it is important to investigate the cause of the water level rise in Lake Awassa. There are two hypothesis explaining the water level rise of the lake:

1) Siltation of the lake by erosion. The focus is on gully erosion due to the formation of great gully systems in the watershed during the last decades.
2) Increase in runoff from the watershed due to for instance the deforestation, causing more water to flow into the lake.

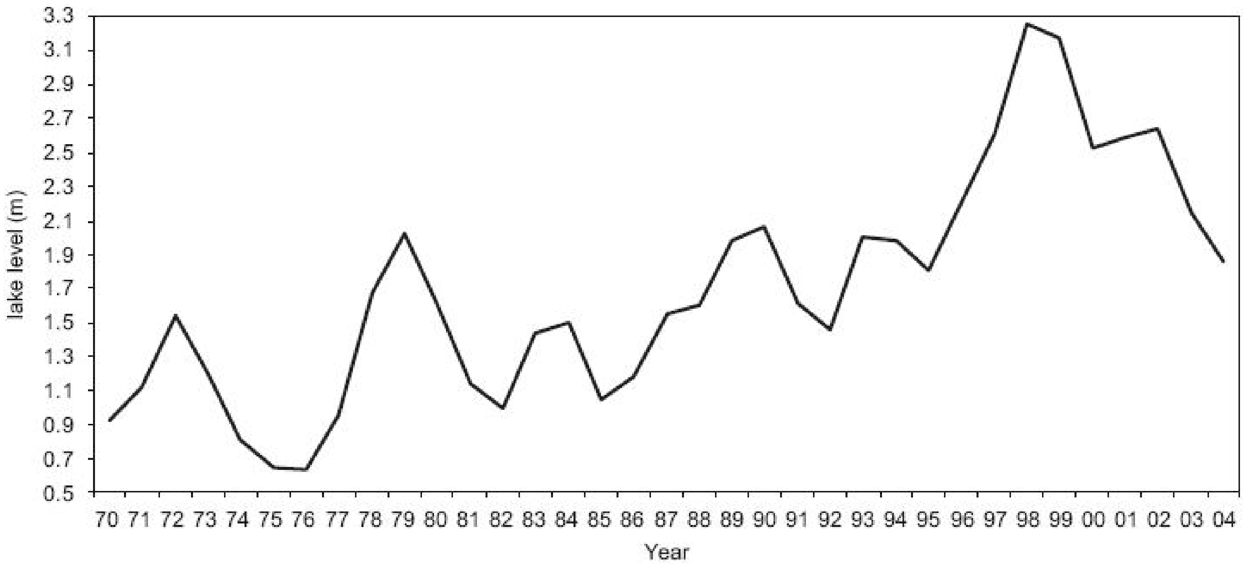

Fig. 1.2. Mean annual lake level fluctuation pattern of Lake Awassa (Abiye 2008).

This Master thesis research focuses on the amounts of sediments caused by gully erosion in a sub catchment of the Awassa watershed, and the addition of those sediments to the Awassa lake. In addition, the changes in land use over the last three decades will be studied and related to the gully erosion. The aim of the study is to determine the contribution of gully erosion to the transport of sediments into Lake Awassa. The following specific objectives have been defined:

- To analyse the changes in land use in the area over the last four decades using available satellite imagery.
- To determine the volumes and sediment losses by the gully systems in a sub catchment of the Awassa watershed.
- To determine the connectivity between the gullies and the Awassa lake.
- To evaluate the effect of the land use changes on gully erosion and input of sediments into lake Awassa.

To achieve these goals, a field survey of two months was carried out in the area from September to October 2012. During this field survey gully dimensions were measured, land use data, soil samples, ground control points and stereo aerial photographs were collected. The aerial photos were used to measure gully dimensions in 1972 and a timeseries of Landsat imagery is used to produce land use maps for the last four decades.

2. Study area

2.1 Lake Awassa

Lake Awassa (Lat: 6°58′–7°8′N; Long: 38°22′–38°27′E) is situated in the Ethiopian Rift Valley which is part of the East African Rift system. The Ethiopian part of this rift system is bordered by Kenya in the south and the Red Sea in the north. The area can be divided into four sub-systems: Lake Turkana (Rudolf) in the south, Chew Bahir, the Main Ethiopian Rift (MER) and the Afar in the north (fig. 2.1.1). The rift has its lowest elevation in the Dalol Depression in northern Afar namely 120 meters below sea level and its highest elevation of 1680 metres above sea level at Lake Awassa (Ayenew 2007).

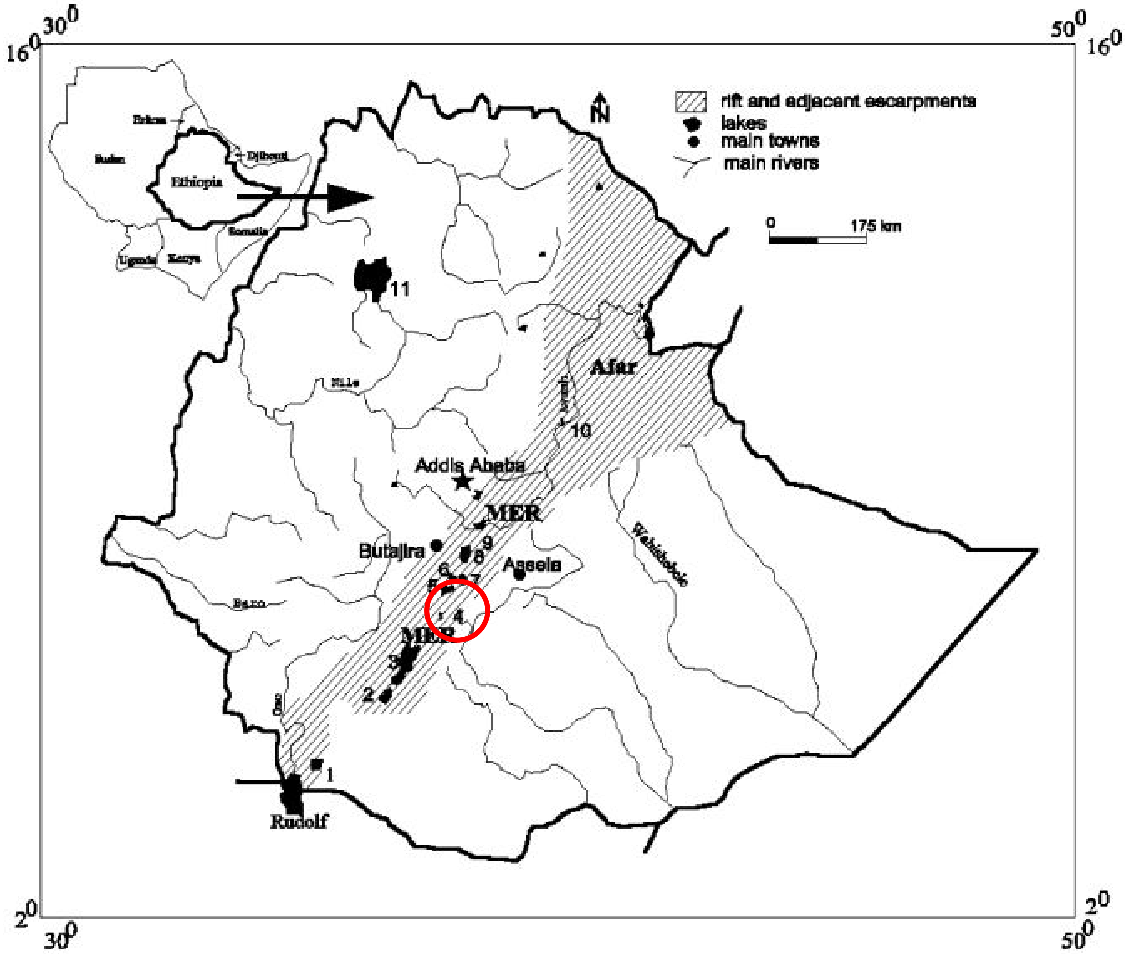

Fig. 2.1.1. Location map, 1: Chew Bihar; 2: Chamo; 3: Abaya; 4: Awassa and Cheleleka; 5: Shala; 6: Abiyata; 7: Langano; 8: Ziway; 9: Koka dam; 10: Beseka; 11: Tana (Ayenew 2004).

The MER contains a series of lakes including Lake Awassa which basin is located within the collapsed Pliocene calderas Awassa and Corbetti (Ayenew et al. 2006). The rift-valley lakes are separated by volcanic hills, basins and volcano-tectonic depressions. The Awassa watershed covers an area of 1455 km^2 containing Lake Awassa and Lake Cheleleka (Shalo) (fig. 2.1.2). Lake Awassa is one of the few freshwater lakes in the MER and has a surface area of about 93 km^2 and a maximum and mean water depth of about 21 and 10 m. Lake Cheleleka had a surface area of 14.5 km^2 and a 63 km^2 area of swamp surrounding it (Telford 2000). Present-day there are only a few small water bodies left where the lake used to be and the rest of the area is covered by swamp. One of the main tributary rivers that feeds Lake Awassa is the Tikur Wuha River which drains Lake Cheleleka. Lake Cheleleka is fed by perennial streams on the north and northeastern sides of the catchment and by runoff from the eastern wall. From the other sides there is no perennial river flow that reaches the lakes. Some of the ephemeral streams reach the lakes, but many of them disappear in wide-open faults before they reach the lakes. There are no rivers draining Lake Awassa and therefore the catchment can be considered as a closed system. The tectonic activity in the area is of great importance to the hydrology of the catchment. Several studies prove that faults and ground cracks play a major role in the substantial transfer of groundwater to the lakes (Tessema 1998, Ayenew 1998, 2001, Ayenew et al. 2004). Lake Awassa has a significantly low salinity for a closed system (Wood et al. 1988) and the groundwater mechanism is suggested as one of the explanations for this.

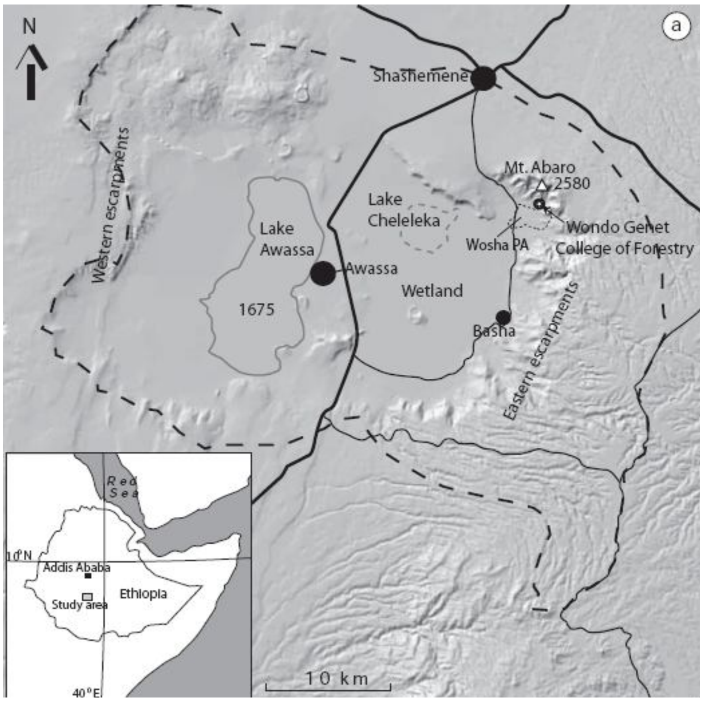

Fig. 2.1.2. Overview of the Awassa watershed, Ethiopia (Dessie 2007).

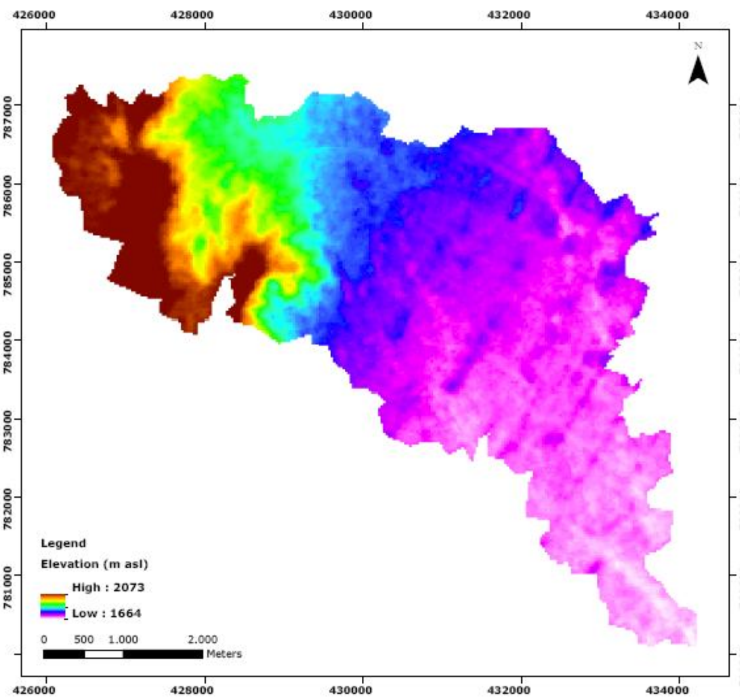

Fig. 2.1.3. Digital Elevation Model of the study area (source: Aster GDEM 2011).

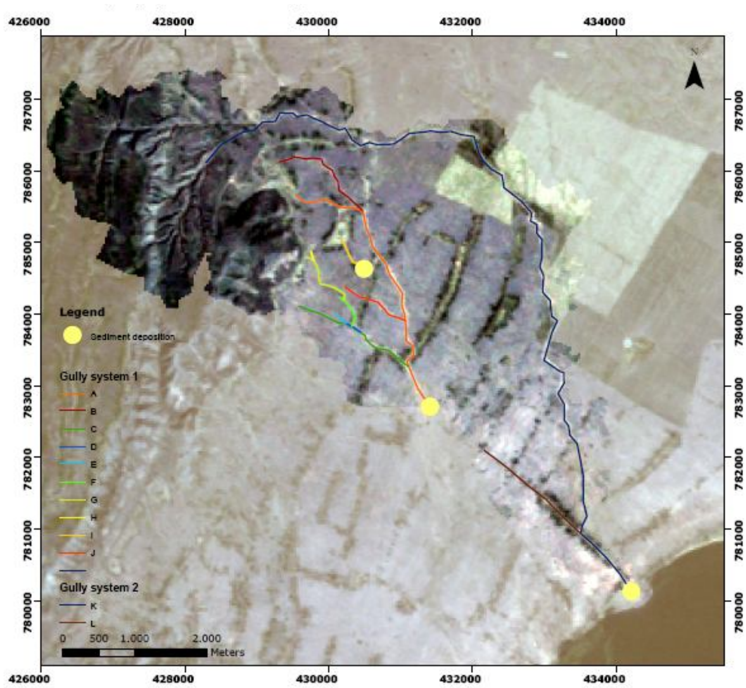

Fig. 2.1.4. Overview of the gully systems and their gullies (source: Landsat 5 TM 2011).

The study area that is chosen is a sub catchment of the Lake Awassa watershed located in the west (appendix A). This is one of the areas that has clearly been affected by gully erosion during the last few decades according to the local people. The elevation varies from 1664 metres in the southeast to 2073 metres in the northwest (see fig. 2.1.3). Clearly visible are the valley plain in the east and the steeper hills in the west. The sub catchment is divided into two smaller sub catchments to separate the gullies that are connected to the lake from the gullies that are not. This results into two gully systems and they contain only classical gullies. Gully system 1 contains the 10 classical gullies A to J with one gully (I) that is not connected to any of the other gullies. The sedimentation areas are located in the middle south of the study area. Gully system 2 contains the two classical gullies K and L and are connected with the lake (see fig. 2.1.4).

2.2 Climate

The Ethiopian Rift Valley has a moist sub-humid to semiarid climate and experiences two contrasting seasons due to the seasonal migration of the Inter-Tropical Convergence Zone (ITCZ). The dry season lasts from November to February and the wet season from March to October with the highest average monthly rainfall from June to September (Degefu 1987). The mean annual precipitation in the Awassa area is about 960 mm which falls in the eight-months-long rainy season (FAO 1984, Gamachu 1977) (see fig. 2.2.1). The overall evapotranspiration exceeds precipitation and the estimated annual pan evaporation ranges from 1600 to 2140 mm (Chernet 1982, Makin et al. 1976, Telford et al. 1999). The mean annual temperature is about 20°C and varies only slightly through the year.

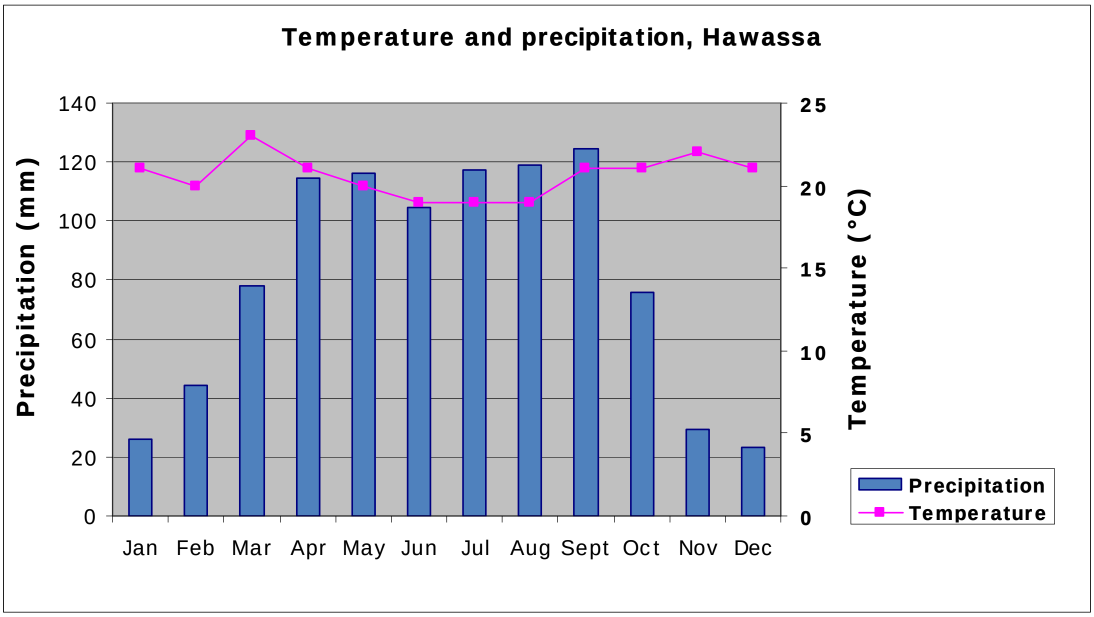

Fig. 2.2.1. Average temperature and precipitation over the year, the precipitation values per month are the averaged precipitation from 1978 to 2007 (source: National Meteorology Agency, Ethiopia).

2.3 Land use and changes

Most of the land in Ethiopia is used for permanent pastures namely 40%. The rest of the land is used for annual crop production 12%, permanent crops 1%, forest and woodland 25% and others 22% (Taddese 2001). A great and important problem in Ethiopia is deforestation (EFAP 1994). This problem is related to socio-political changes, economic activities, population growth, cultural patterns, agricultural development and local conflicts over resources (Dessie 2007). The total global annual forest loss is 9.4 million ha (FAO 2000) and in Ethiopia the forest cover has decreased to less than 3-3.6% in the past half-century (Reusing 1998, WBISPP 2004).

There are two major towns Hawassa and Shashemene which are growing at rates of 2.1% and 4.1% respectively (CSA 1996). One third of the population, about 0.3 million people live in these towns. People use the land in the surrounding area for agriculture and in average each household owns less than one hectare of land.

The vegetation cover in an area is influenced by altitude, rainfall and soil fertility. The eastern part of the Awassa watershed is wet and the dominant vegetation type in this area is montane forest composed of Podocarpus falcatus and Juniperus procera (Russ 1944). In the western part the climate is more sub-humid and shrubs and thickets dominate here (Chernet 1982). The remaining foot-slopes and valley floor are covered by grassland, bush land and acacia woodland. The forest on the eastern rift flank used to be more extensive and coherent than it is now. The major crops in the area consists of enset (banana plant), khat, sugarcane, maize and potatoes and irrigation farming dominates in the flat and undulating site of Wondo Genet. There are two main crop seasons in Ethiopia the 'belg' and 'meher' seasons. The belg season is from February to June and is official defined as any crop harvested between March and August. The meher season is from June to October and is defined as any crop harvested between September and February. The greatest production is during the meher season and produces 90-95% of the total cereals output and the belg season produces the remaining 5-10% (USDA 2008). The enset, also known as 'false banana' is one of the three genera in the banana family, but is used for its roots and is Ethiopia's most important root crop. It takes four to five years for the plant to mature and therefore to harvest in every season the planting needs to be staggered over time. The plants are quite drought tolerant, more than most cereal crops. Khat plants can grow under broad climate conditions and tolerate drought for a long time. Besides that, khat can be harvested throughout the year (Dessie et al. 2007b). In the southwest of Ethiopia, maize is planted between early May and June and is harvested in late December to mid-January. The plant is cold intolerant and requires an altitude of up to 2,400 metres above sea level and rainfall between 800 and 1,500 mm for higher production (ECX 2012). Awassa is one of the largest potato producing areas of Ethiopia. They are mainly planted during the peak rains in the meher season and they are usually grown in a multicropping or rotational system (Borgel et al. 1980, Medhin et al., 2001). In the study area the major crop is maize which is harvested in late October to November. In this area there is only one crop season, the meher season. Besides maize there are a few parcels with enset and one parcel where aloe vera is grown.

The expansion of agriculture in the Awassa watershed due to the growing population caused over 80% of the forest area loss. Over 40,000 ha of natural forest was lost in the period between 1972 and 2000, which is over 80% of the forest cover that was present in 1972 (fig. 2.3.1). This is equal to about 1400 ha of annual forest loss which is 0.9% of the annual national forest loss (Dessie et al. 2007a). Deforestation causes a decrease in infiltration rate of the soils leading to a higher runoff and thus higher soil erosion rates by water. The deforestation and especially the irrigation of the land could have caused the drying out of Lake Cheleleka by decreasing the stream flow.

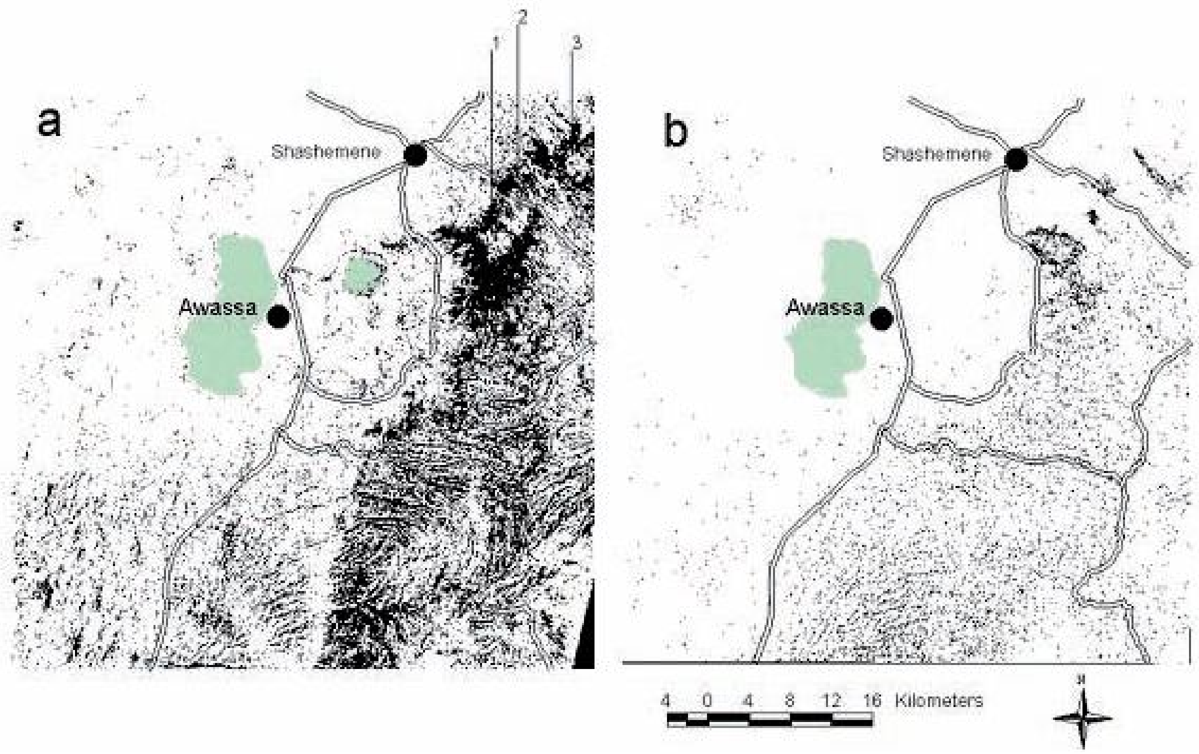

Fig. 2.3.1. Interpreted satellite images from 1972 (a) and 2000 (b) showing forest cover, black color, in the study area during those periods. The year 2000 image shows significant decrease of forest cover and the drying out (disappearance) of Lake Cheleleka, grey color, in comparison to year 1972 (Dessie 2007).

2.3.1 Vegetation recovery and other measures to prevent erosion

People recognize the problems that come with the deforestation. The slopes of the hills in the study area were used for grazing by cattle for decades. According to the local citizens and university staff the access to this hills has been closed for cattle since about 5 years in order to recover the vegetation. Projects emerge with the plan to grow tree species that used to grow in the area in a nursery and plant them in the area when they have grown sufficiently to survive. The vegetation recovery has the goal to improve the water infiltration into the soil to decrease the runoff and thus the erosion by water.

Vegetation is also used to prevent further gully erosion in the area. In most of the gully heads vegetation is grown since a few years and fences are placed to stabilize the gully head (fig. 2.3.2). Besides that there are barriers of small cacti planted in the gullies and in a part of gully K aloe vera is used as such (fig. 2.3.3 and 2.3.4). Behind these barriers small vegetation is grown such a grasses.

Another measure to reduce water erosion that can be found in the study area are trenches (fig. 2.3.5). Trenches are constructed in a way that they run perpendicular to the flow of the water. Their purpose is to reduce the flow velocity and promote the infiltration into the soil.

Fig. 2.3.2. Vegetation and barriers in the gully.

Fig. 2.3.3. Barriers of small cacti.

Fig. 2.3.4 Barriers of aloe vera.

Fig. 2.3.5. Trenches constructed perpendicular to the water flow.

2.4 Soil

The Ethiopian Rift Valley is characterized by tectonic and volcanic activity with several shield volcanoes developed over the adjacent plateaux. The rift itself is covered with Cenozoic volcanic and sedimentary rocks (Ayenew 2007). The volcanic activity is expressed in the soil layers in the study area and visible in the walls of the gullies (fig. 2.4.1 and 2.4.2). The topsoil in the study area consists of sandy loam with a thickness varying from a few tens of centimetres up to 3 m. Underneath the sandy loam a layer of volcanic ash can be found, this layer has an average thickness of about 1.5 m. The volcanic ash is light material and is easy erodible. Therefore, when this layer is reached the erosion increases. The volcanic ash floats in the water and erodes easier than the sandy loam top layer which results in undercutting of this layer. Eventually the gully wall becomes unstable and collapses and subsequently will the soil be transported downstream by the water. In the upstream area where the gullies are deeper, another sandy loam layer is visible underneath the volcanic ash layer.

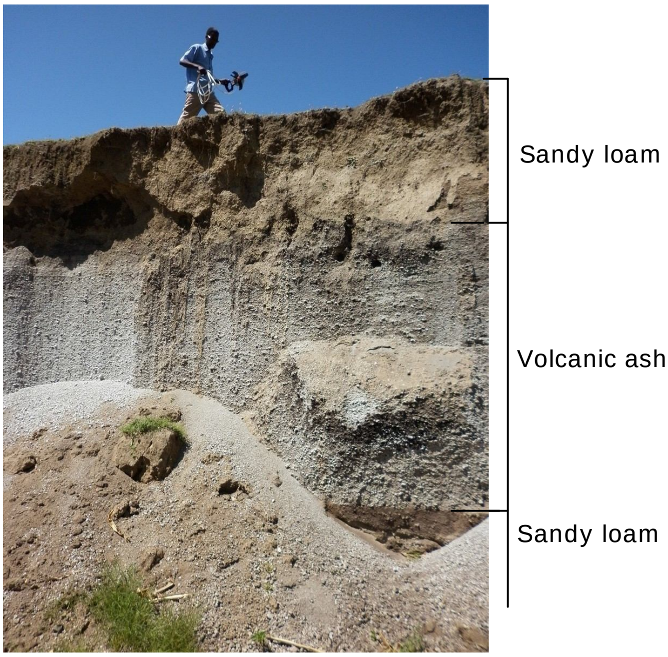

Fig. 2.4.1 and 2.4.2. Different soil layers visible in the gully walls in the study area.

The sediment that is transported through the gullies in the study area consists mainly of sandy loam and volcanic ash. The volcanic ash is more vulnerable for erosion and gully formation than the sandy loam and is easily transported by water. Therefore this material may have potentially a high sediment yield into the lake.

3. Methodology

3.1 Selection of the study area

The study area is chosen by visually comparing of the gully erosion visible on the SPOT images of 2006/2007 and on the aerial photographs of November 22, 1972. The goal was to find areas where significant changes occurred in gully erosion during the last 40 years. The local people, university staff and local citizens, pointed out that gully erosion mainly occurred in the western area of the Awassa watershed which is in agreement with the changes that are visible when comparing the satellite images with the aerial photographs. After discussion with the local people only one area turned out to be accessible. Due to this there was decided to focus in more detail on that area, a sub catchment of the Awassa watershed. To determine the exact borders of the sub catchment the Aster GDEM is used and processed in ArcGIS 10.

3.2 Aerial photos and satellite imagery

The imagery used in this research comprise: three Landsat 5 TM images of December 23, 1986, December 13, 1994 and January 10, 2011, the Aster GDEM version 2, a SPOT 5 image of 2006-2007 and three stereo aerial photographs of November 22, 1972 with an overlap of 60%. The SPOT 5 image and the aerial photos were obtained at the Ethiopian Mapping Agency located in Addis Ababa, Ethiopia. An overview of the characteristics of the imagery is presented in table 3.2.1 and 3.2.2.

Sensor	**Band Number**	**µm**	**Resolution**	**Image data**
Landsat 5 TM	1	Blue: 0.45-0.52	30 m	December 23, 1986
	2	Green: 0.52-0.60	30 m	December 13, 1994
	3	Red: 0.63-0.69	30 m	January 10, 2011
	4	NIR: 0.76-0.90	30 m	
	5	SWIR: 1.55-1.75	30 m	
	7	SWIR: 2.08-2.35	30 m	
Aster GDEM V2			30 m	October 17, 2011
SPOT 5	1	Green: 0.50-0.59	5 m	2006-2007
	2	Red: 0.61-0.68	5 m	
	3	NIR: 0.79-0.89	5 m	

Table 3.2.1. Characteristics of the satellite imagery

Aerial photos 1972	
Scale	1:50000
Format (cm)	23 x 23
Focal length (mm)	152.05
Date	22 November

Table 3.2.2. Characteristics of the aerial photos.

The Landsat 5 TM images are all taken in the dry season which is necessary to be able to compare the land use over time. Preferable is to obtain imagery of the same months as when the fieldwork is carried out to be able to compare the collected field data with the most recent image. Field measurements were done in the first months of the dry season and the only available Landsat data of the early dry season is the imagery used in this research. There should be taken into account that the gathered land use data in the field is collected in October while the 2011 Landsat image is taken in January. This is about three months later in the dry season and thus the vegetation will be dried out more and crops could be harvested by that time. The aerial photos are taken in the end of November while the field survey is carried out in September to October. However, during the field survey in October when the gully dimensions where measured the rainy season was already to an end and there was no significant water erosion taking place anymore.

3.3 Land use classification

To link the gully erosion with land use changes, the collected Landsat images need to be classified. To get an accurate classification the land use maps need to be validated by collecting ground control points in the field which is done with a Garmin GPS 72H with and average accuracy of 5 metres. The most important areas that are exposed to land use changes are in this case the areas around the gullies and in the upstream area. Vegetation changes in these areas affect the hydrology which could lead to a decrease or increase in soil erosion by water. In total 28 ground control points are collected and processed in Excel and plotted as a shapefile in ArcGIS including the land use descriptions (appendix D). The gathered data could in this form easily be used to validate the classified image of January 2011.

The study area is extracted from the three Landsat images in ArcGIS before classification of the land use. Different classifications were performed on the images in Erdas 2011 and ArcGIS 10. To determine the accuracy of the produced land use maps, the land use map of 2011 is compared with the collected ground control points. A land use map has the highest accuracy when all the collected ground control points are classified correctly. The best results are obtained with the unsupervised classification in Erdas 2011 using signature files. This means that the observed land use in the field is classified best with this method. There is chosen for 4 classes to distinguish the main land use types based on observations in the field. In the mountains dense vegetation is observed that consists of trees and bushes, further down slope the vegetation becomes less dense and consists of bushes and grasses of medium height. In the plain area bare soil dominates, several grassland areas can be distinguished and trees and bushes are found along the roads. Four classes is the minimum amount of classes needed to correctly classify bare soil and the different types of vegetation in the area. When more classes were used to distinguish more vegetation types, several areas of bare soil were classified as vegetation which made the land use maps less accurate than when 4 classes were used. The classes that are used are bushes and trees, medium high grasses and bushes, low grasses and bare soil.

3.4 Measuring gully erosion

There are several methods to estimate soil loss by gully erosion (Poesen et al. 2003). To determine this, first the volume (m^3) of the studied gullies needs to be calculated by measuring the gully length, width and depth at several places. These measurements are then averaged to get an estimation of the volume using the following equation:

$$V = \sum_{i-1}^{n} L_i A_i \quad (1)$$

Where L_i is the length of the gully segment in metres and A_i is the cross sectional area of the gully segment in m^2 (Nyssen et al. 2006). With the calculated volume the area-specific long-term gully erosion rate (R_L) in t $ha^{-1}y^{-1}$ can be calculated.

$$R_L = \frac{VBd}{TC} \quad (2)$$

$$R_S = \frac{(V - V_0)Bd}{TC} \quad (3)$$

Where R_s is the area-specific short-term gully erosion rate (t $ha^{-1}y^{-1}$), V_0 is the initial gully volume at the beginning of the considered time span (m^3), Bd is the average bulk density of the soils occurring in the contributing area (t m^{-3}), T is the time span considered (years) and C is the watershed area (ha) (Nyssen et al. 2006). For this research there has been chosen to use ground-based and airborne techniques to estimate the gully volumes and gully erosion rates.

3.4.1 Measuring gully dimensions in the field

To determine the recent volumes and total sediment loss of the gully systems a field survey was carried out in the months September and October 2012. In this period several gully profiles were measured and soil data was collected to eventually determine the sediment yield by gully erosion. An overview of the collected data can be find in appendix B.

<u>Volume calculation</u>

Measuring gully dimensions in the field can be performed in different ways. One basic method is measuring gully profiles with levelling equipment. The levelling instrument has to be placed perpendicular and a few metres from the gully, so that the first reading can be carried out at the gully wall (fig. 3.4.1). There will be carried out as many readings as necessary to obtain an accurate profile. This method was the first plan to accurately measure gully dimensions in the field. However, after field observations this method turned out to be inefficient due to extreme depths in the upstream area that were greater than the available levelling rod.

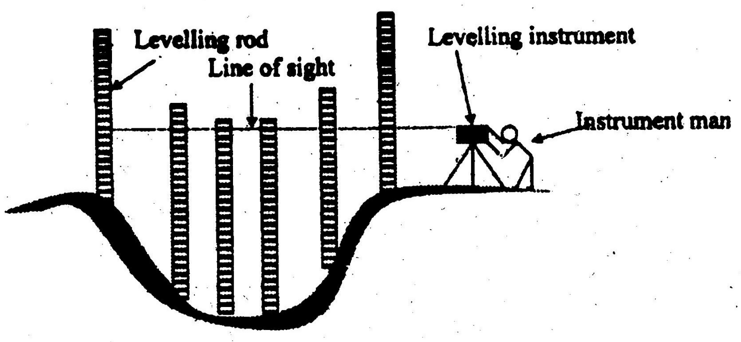

Fig. 3.4.1. Measuring the profile of a gully (Tulu 2011).

A more basic but also efficient method in this study area is using measuring tape (fig. 3.4.2). The gully profiles were in overall rectangular shaped and therefore only the depth and one width were measured. For practical reasons there was chosen to measure the bottom width. The distances between the profiles were not fixed, but there was tried to spread out the measurements throughout the gully to give a good overview. More measurements were done with increasing changes in width and/or depth of the gully. An overview of the measured profiles per gully can be find in appendix C. In total there were 49 profiles measured in gully system 1 and 38 in system 2. The subdivision of the gullies is done in the field by giving every new tributary a different name. The results of the profile measurements were processed in Excel and the widths and depths were used to obtain the area per profile and the width-depth ratio. Moges et al. (2008) concluded that an increase in the width-depth ratio is an indication for a decline in flow rate and slope angle and could thus indicate potential sedimentation.

Fig. 3.4.2. Using measuring tape to measure gully dimensions in the field.

The distances between the profiles were calculated in GPSTrackMaker and ArcGIS 10 and were not measured in the field. At every profile a GPS point was taken with a Garming GPS 72H and processed in GPSTrackMaker and ArcGIS 10. In case of a difference in distance calculated by both programs, the most likely distance was used or the results were averaged. For the volume calculation there is assumed that the calculated area of a profile represents the area of the gully until half the distance to the next profile point. Therefore the distances needed to be recalculated and this is clarified in figure 3.4.3. With the new results the volumes per gully section were calculated in Excel and added to get the total volume per gully and gully system. In the results a difference is made between the gully erosion rate of gully system 1 including and excluding gully I. Gully I is included to give the total gully erosion rate of the sub catchment of gully system 1. However, gully I is not connected with other gullies and has a different sedimentation area. By excluding gully I in the calculations the gully erosion rate for the gullies A to H and J and their sedimentation area is obtained.

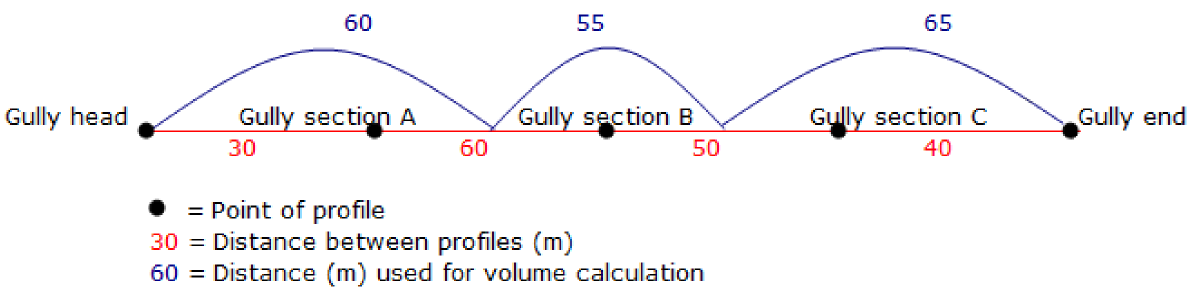

Fig. 3.4.3. Calculation of the lengths per gully sections.

Soil sampling

Soil sampling was necessary to obtain the dry bulk density of the main soils in the area to calculate the sediment yield of the gullies. The dry bulk density (ρ_d) in g cm^{-3} is expressed by the following equation:

$$\rho_d = \frac{M_s}{V_t} \quad (4)$$

Where M_s is the mass of the dry sample (g) and V_t is the total volume (volume of the wet sample) in cm^3. Samples were taken in the gully walls with kopecky rings with a fixed volume of 100 cm^3. The samples were taken spread out through the area and gullies and only the main occurring soils were sampled. In total 19 samples were taken, 13 samples at 6 places in gully system 1 and 6 samples at 4 places in gully systems 2 (appendix D). To obtain the dry weight of the soil samples, the samples were oven dried at 105 degrees Celsius for 24 hours. The results were processed in Excel and the outcomes were used to calculate an average dry bulk density for every gully.

Time span and watershed area

The gully dimensions are measured in the field in 2012 and the results are compared with the results of the measurements with stereo aerial photography with photos from 1972. This is a comparison of gully development over 40 years, therefore the considered time span is 40 years.

As mentioned before, the Aster GDEM is used and processed in ArcGIS 10 to determine the exact borders of the sub catchment. This is established by using the hydrology toolset within the spatial analyst tools to calculate the watershed. This same method is used to calculate the watershed areas of gully system 1 and 2. The amount of pixels per watershed were then multiplied with the resolution of the pixels of the Aster GDEM and converted to hectares.

3.4.2 Measuring gully dimensions with stereo aerial photography

Airborne techniques can also be used to determine the volume and sediment loss by gully erosion, but only for gullies that are visible on the used images so high resolution imagery is required (Poesen et al. 2003). High resolution satellite images are available and are proved to be useful in the assessment of gully erosion (Vrieling, 2007), but they are only available of about the last 20 years. Over a longer time scale aerial photographs are available, therefore they will be used for this study. To calculate the volume and sediment loss a digital terrain model (DTM) needs to be created of the obtained stereo aerial photographs of November 22, 1972.

The obtained aerial photos are analog and need to be digitized and geo-referenced before a DTM can be created. The photos are scanned at 2300 dpi for high resolution pixels and are further processed in Erdas 2011. To geo-reference the images ground control points were collected in the field with a Garmin GPS 72H, with the SPOT image in ArcGIS and Google Earth. The last two collection methods are used to obtain points in the inaccessible areas and to get a significant variation in x, y and z coordinates throughout the area to enhance the DTM. The aerial photos were compared with the SPOT image to locate road intersections and bends that could be used as GCP. Due to great changes in infrastructure over the last 40 years, gully intersections are used as well. In total 10 ground control points are collected with the Garmin GPS with an average accuracy of 5 metres and 6 with the SPOT image and Google Earth. The final step in the creation of a DTM in Erdas is the Automatic Terrain Extraction (ATE). When measuring gully dimensions with aerial photos it is important to create a high quality DTM with a high resolution. At this point there are two options to create the DTM in Erdas, namely using the ATE or the enhanced Automatic Terrain Extraction (eATE). The ATE has a shorter calculation time and to obtain the first results this option is chosen. The eATE process is also used to create a DTM to determine which process gives the best results.

In this process the lake area is masked and extracted from the image to avoid errors in this area. To evaluate if a DTM with a higher quality could be created the software Agisoft PhotoScan Professional is used. After loading the photos in the program the images are geo-referenced with the gathered ground control points like in the program Erdas. When this is the done the program can build the geometry by itself and generate an orthophoto.

The next step is to measure the gully dimensions and calculate the volumes. This step has not been carried out due to the inability to create a DTM of sufficient quality. However, the idea was to create a trend surface and subtract the DTM from this surface. The result will be a surface representing the erosion that took place and thus the gullies that were already there in 1972. The software Agisoft PhotoScan Professional would have been used to measure the gully dimensions to calculate the volumes. The dry bulk densities that are measured in the field would have been averaged to calculate the gully erosion rate in 1972.

3.5 Determining the gully activity and connectivity with the lake

There are two observations that have to be made to determine if a gully is contributing to siltation of the lake. The first observation is the activity of the gully and the second is the connectivity of the gully with the lake. According to the rule by Oostwoud et al. (2000) a gully is active if at least one of the following is observed:

1) Undercut or plunge pool causing cave-in
2) A vertical or nearly vertical wall
3) No vegetation on the gully wall
4) Tension cracks
5) Side wall collapse and sediment on the gully floor

The rule is used in the field to decide if a gully is active or not. The connectivity of a gully with the lake is simply determined by following the gully to its sedimentation area.

4. Results

4.1 Field data

During the fieldwork the size and extend of the gullies were mapped and observed. Remarkable in the study area is the size of the gullies varying in width between 2 and 76 m and in depth between 1 and 11 m. The longest gully is gully K with a length of almost 13 km. The gullies that are developed in the plain part of the area are wide enough to be used as roads, which is thus done by the local people and their cattle. The gully dimensions in the hills where the slopes are steeper are smaller and deeper than the ones in the plain area where the gullies are wide and shallow. The gathered field data is described in this paragraph per gully system.

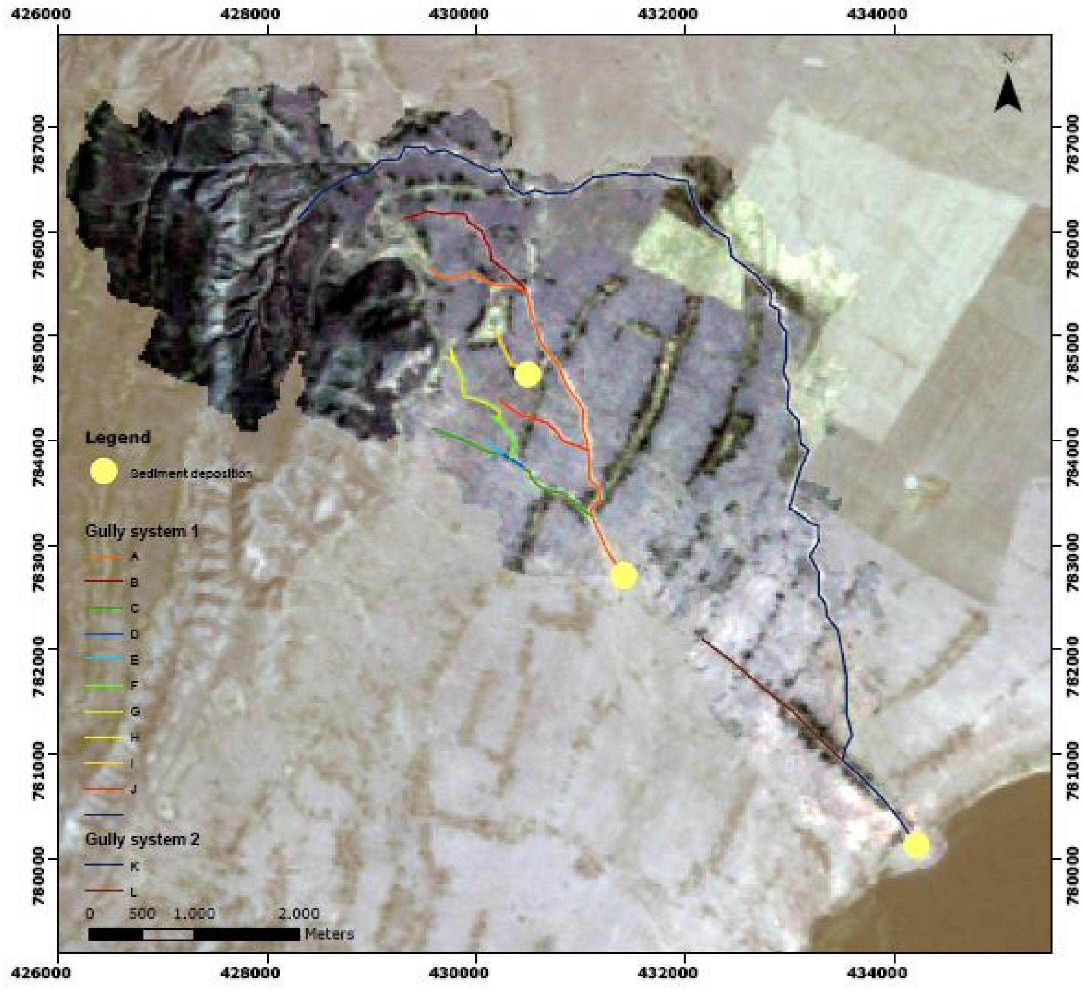

Fig. 4.1.1. Overview of the gully systems and their gullies (source: Landsat 5 TM 2011).

<u>Gully system 1</u>

As described before, gully system 1 consists of 10 gullies from which 9 are connected to each other and one gully I is not. An overview of the gullies and their sedimentation areas as observed in the field are shown in figure 4.1.1 for gully system 1. One main question can already be answered with this figure, namely if the gullies are connected to the lake. The figure shows clearly that the sedimentation area of the 9 connected gullies is located in the middle south of the study area about 3.8 km from the lake. The sedimentation area of gully I lies even further land inwards. The second important observation is the activity of the gullies. According to the rules by Oostwoud et al. (2000) described in the methodology section, the 9 gullies A to I can be defined as active gullies. The activity is visible by side wall collapse and sediment on the gully floor, a vertical or nearly vertical wall and undercutting of the gully wall. Gully J turned out to be different than the other gullies in the area, as in that it has a high vegetation rate in comparison with the others (fig. 4.1.2 and 4.1.3). However, when observing the gully closely there are parts visible that are active in the form of side wall collapses and undercutting of the gully wall. At the gully head both forms are clearly visible which indicates that also this gully is active (figure 4.1.4).


Fig. 4.1.2 and 4.1.3. Vegetation in gully J.

Fig. 4.1.4. Activity at the gully head of gully J.

For each gully the total length, volume and dry bulk density are calculated (table 4.1.1). The dry bulk density is calculated for each gully separately based on the outcomes of the collected samples. Soil samples were taken in the gullies A, B, H and I and for each of the four gullies the dry bulk density was averaged and used. For the other gullies the averaged value of the bulk densities for gullies A, H and I are used. The soil around those gullies give the best representation of the soil around the other gullies. The total length of all the gullies in this gully system is 13.4 km with a total volume of 965000 m^3. Assuming that the gullies developed in the last 40 years, the area-specific long-term gully erosion rate is 23.4 t $ha^{-1}y^{-1}$. Considering that gully I is not connected with the rest, the gully erosion rate for the sedimentation area in the middle south is 22.9 t $ha^{-1}y^{-1}$.

Gully	Total lenght (m)	V	Bd	V*Bd (t)	T	C	R_L
A	4845	527749	0.724	381915			
B	1828	106261	0.829	88091			
C	2581	151795	0.751	114015			
D	129	3773	0.751	2834			
E	275	4648	0.751	3491			
F	714	38650	0.751	29030			
G	1165	49336	0.751	37057			
H	224	8960	0.742	6651			
I	598	20884	0.787	16443			
J	1047	52881	0.751	39720			
Gully system 1	**13400**	**965000**		**719000**	**40**	**769**	**23.4**
Without gully I				**703000**			**22.9**
K	12820	1734696	0.886	1537230			
L	1882	43793	0.969	42436			
Gully system 2	**14700**	**1778000**		**1580000**	**40**	**1913**	**20.7**

$$R_L = \frac{VBd}{TC}$$

R_L is the area-specific long-term gully erosion rate (t $ha^{-1}y^{-1}$)
V is volume of the gully (m^3)
Bd is the average dry bulk density of the soils occurring in the contributing area (t m^{-3})
T is the time span considered (years)
C is the watershed area (ha)

Table 4.1.1. Length and volume per gully and results of the calculation of the gully erosion rate.

<u>Gully system 2</u>

An overview of the gullies in gully system 2 are shown in (fig. 4.1.1). Noticeable in this figure is that the system contains only two gullies including the longest one named gully K showed in blue. This gully has a total length of about 12.8 km and is the longest gully in the study area. Gullies K and L are connected and what also can be seen in the figure is that their sedimentation area is in Lake Awassa. After field observations and applying the activity rules both gullies are defined active. In both gullies wall collapses can be find as well as undercutting of the gully wall and nearly vertical to vertical walls.

Also for these gullies the total length, volume and dry bulk density area calculated and outlined in table 4.1.1. Soil samples were taken in each gully, resulting in the averaged dry bulk densities values shown in the table. The total length of both gullies is 14.7 km and the total volume is 1778000 m^3. The watershed area of this gully system is about 2.5 times the size of the area of gully system 1. This results in a area-specific long-term gully erosion rate of 20.7 t $ha^{-1}y^{-1}$, slightly lower than the gully erosion rate of system 1.

<u>Width-depth ratio</u>

For the gullies A, B, C, G, I and J of gully system 1 and the gullies K and L of gully system 2 the width-depth ratio is calculated (fig. 4.1.5 and 4.1.6). The other gullies have too few width and depth measurements for a representative width-depth ratio graph. The values for the width-depth ratio vary between almost 0 to 36. The graphs show that for all gullies except gully L holds that the width-depth ratio increases towards the gully head to a value below 5. In gully system 1 the gullies A and C show great difference in values with a maximum around 36 in the downstream area that increases suddenly below 5 towards the gully head. Gullies B, G, I and J have their maxima below 13 and show a gradual decrease towards the gully head. Noticeable for gully B is the sudden increasing value from 2 to 7 at 950 m. In gully system 2 the transitions in width-depth ratios of the gullies are less gradual than in gully system 1. The width-depth ratio of gully

L seems to increase towards the gully head. However, when excluding the last point the average width-depth ratio is about 9. The graph of gully K shows values above 10 between a distance of about 3 and 10 km that decrease again below 10 after 10 km distance. This gully shows the most variation in width-depth ratios. According to Moges et al. (2008) high width-depth ratio values indicate a decline in flow rate and potential sedimentation. For gully I there is known that at the end of it sedimentation takes place, this is shown in the graph by a sudden increase in the width-depth ratio to about 12.5. Sudden increases can also be found in the width-depth ratios of the gullies A, C, K and L.

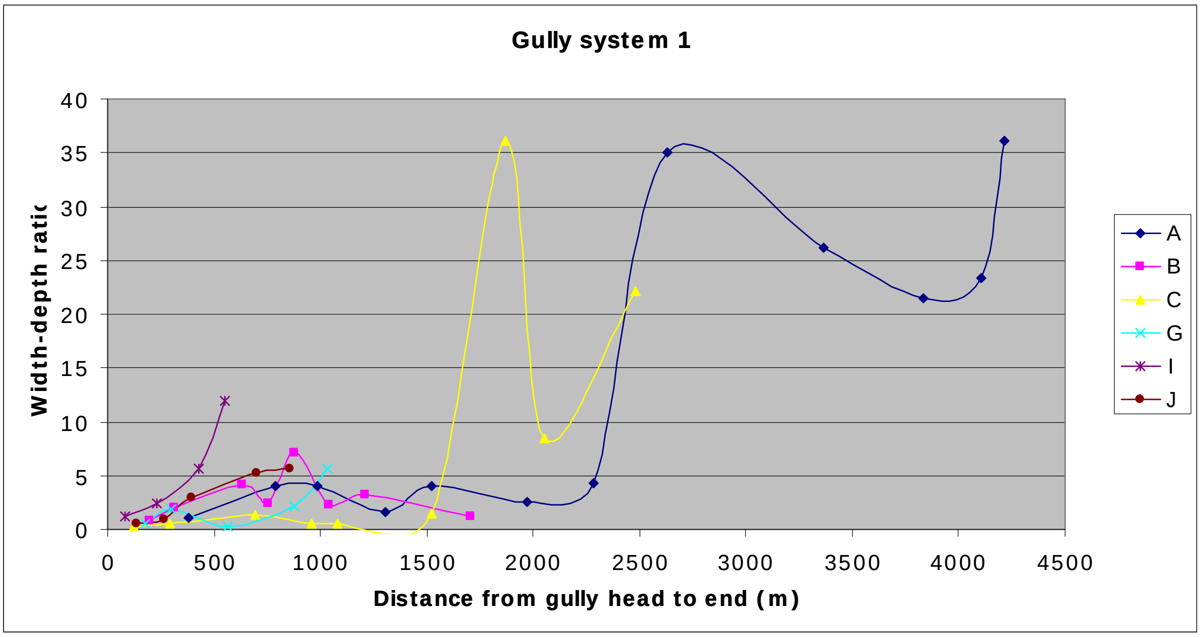

Fig. 4.1.5. Width-depth ratios for the gullies A, B, C, G, I and J of gully system 1.

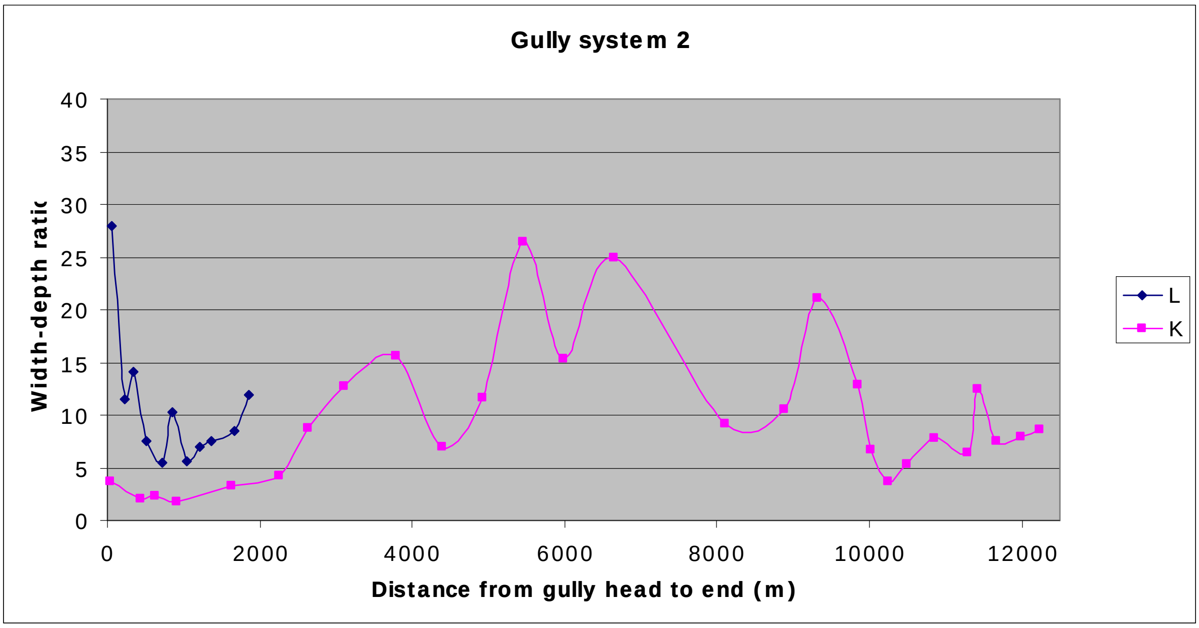

Fig. 4.1.6. Width-depth ratios for the gullies K and L of gully system 2.

4.2 Stereo aerial photography

Results of the DTM creation with Erdas and Agisoft Photoscan

The printed material of the obtained analog aerial photographs turned out to be a problem when digitizing the photos. The result of a scanned photo is shown in figure 4.2.1, where part of the photo is zoomed in to reveal the problem. The digitized photos show a regular pattern of small hooks that is not visible on the analog photos. Several scanning options were used to minimize the visibility of the pattern with the best result shown in the figure.

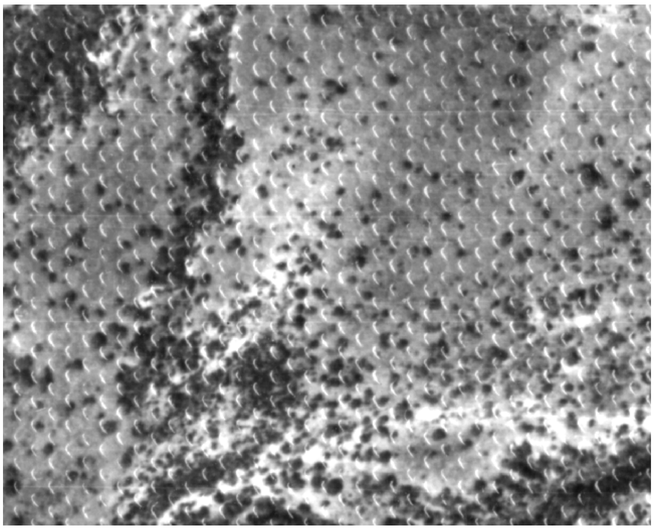

Fig. 4.2.1. Result of a part of one of the digitized aerial photographs, showing the hook pattern.

The digitized photos, even though there is still a hook pattern visible are used to create the digital terrain model in Erdas 2011 and in Agisoft Photoscan Professional. The resulting DTMs are shown in figure 4.2.2 and 4.2.3. Figure 4.2.2 shows the result after the eATE process in Erdas, but only the northern part of the area. The results after the ATE process are not of sufficient quality to reveal the gully pattern that is necessary to perform gully dimension measurements. Therefore the eATE process is chosen to create the final DTM. The DTM has a resolution of 10 m based on the accuracy of the collected ground control points. This part of the DTM is already adjusted in ArcGIS by removing the edges of the image and calculated points that do not fit in the natural landscape to reduce the noise in the image. Even after these adjustments the image still contains noise. The image shows clearly the mountains in the west and the plain area towards the lake to the east. However, when observing the DTM more closely a gully pattern cannot be recognized which makes this image unusable for measuring gully dimensions. The other figure shows the result after processing the photo in Agisoft Photoscan. The resolution of this DTM is 1.1832 m which needs to be adjusted to the accuracy of the ground control points before it can be used. The image shows more gradual transitions than the other image and the mountains in the east area are clearly visible. There are great errors in the east due to the lake area that has not been extracted from the image. Similar errors were visible in the other DTM in the lake area before it was removed. Besides the clearly visible mountains there are also no gully patterns visible in this image. Therefore there can be concluded that it was not possible to create a DTM of sufficient quality to perform accurate gully dimension measurements with stereo aerial photography.

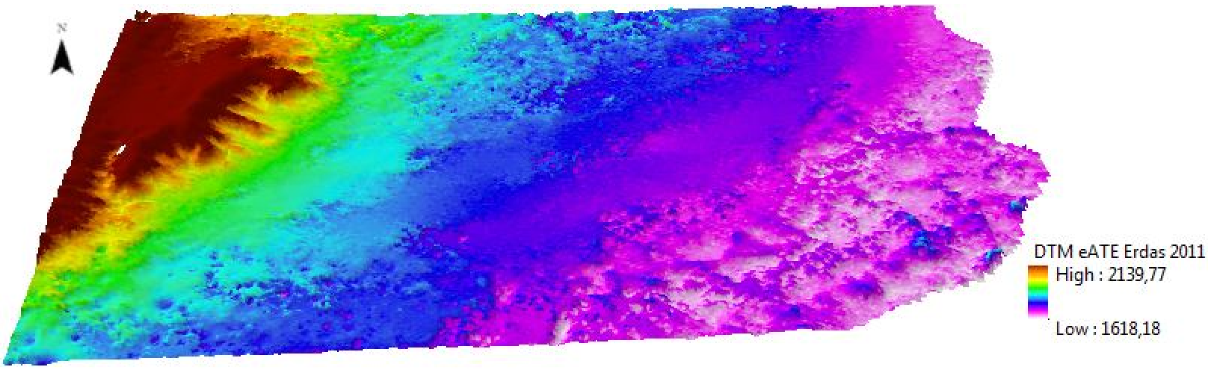

Fig. 4.2.2. DTM result after being processed in Erdas 2011, using the eATE process.

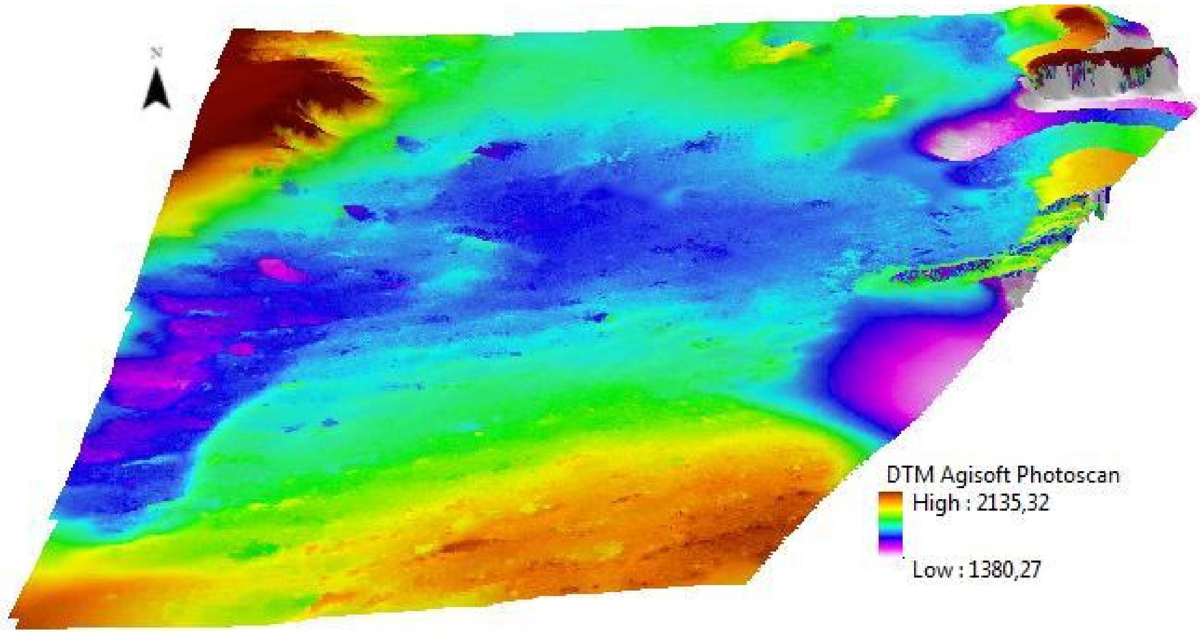

Fig. 4.2.3. DTM result after being processed in Agisoft Photoscan Professional.

<u>Visual evaluation of the aerial photos</u>

There are two other options to obtain information about the gully dimensions in 1972 from the aerial photos. The first option is to visually evaluate the photos in 3D in the Stereo Analyst module of the Erdas program. This module has a measuring toolset to measure the length, width and depth of the gullies to be able to calculate the volume of the gullies. The second option is to create an orthophoto of the area in 1972 and compare this image visually with the SPOT image of 2006/2007 for its resolution and the present gully network. In this case only the change in length of the gully over time can be evaluated. Through this way an estimation can be given of the percentage in gully length that was already there in 1972. Assuming that the width and depth does not change over time the maximum volume of the gullies in 1972 can be estimated. With this data the minimum volume change over the last 40 years can be calculated.

The 3D view in the Stereo Analyst module gives an overall view of the height differences in the study area. There is clearly a depression visible in the landscape at the gully head of gully K that continuous to the east. When zooming in to evaluate the rest of the gullies the 3D view turns bad which is caused by the hook pattern in the image. Accurate gully dimension measurements could not be carried out due to this.

The last option is to visually estimate the gully lengths in 1972. The result of the geo-referenced aerial photos is shown in figure 4.2.4. In figure 4.2.5 the same photos are shown including the present gully systems and their sedimentation areas. When comparing these two images there can be seen that the present gullies were not all there in 1972. After comparing them more closely, there can be said with certainty that parts of gully A, B, J and K were already there in 1972. The results of this comparison are shown in figure 4.2.6. After measuring the lengths it turns out that most of gully B, namely 1340 m of its length was already there which is about 73 percent. About 54% of the length of gully J can be find in the photo, about 38% of gully K and 7% of gully A (table 4.2.1). This means that about 15% of the total volume of gully system 1 was present in 1972 and about 37% of gully system 2. Taking both gully systems together this means that at least 50% of all the gullies in the study area were developed in the last 40 years. Assuming that the width and depth did not change, an estimation is made of the volumes of the gullies in 1972 according to their lengths in 1972 and their volumes in 2012 (table 4). This results in an area-specific short-term gully erosion rate of 19.7 t $ha^{-1}y^{-1}$ for gully system 1 and a gully erosion rate of 13 t $ha^{-1}y^{-1}$ for gully system 2.

Fig. 4.2.4. Result of the geo-referenced aerial photographs (source: aerial photos 1972, Ethiopian Mapping Agency).

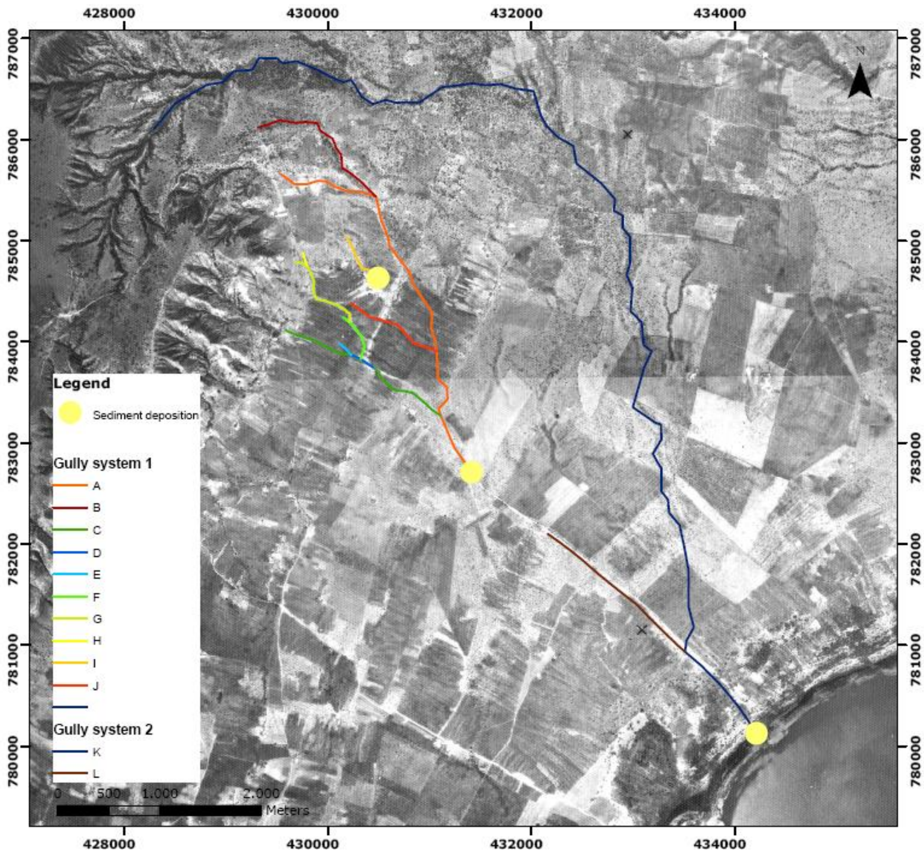

Fig. 4.2.5. The geo-referenced aerial photographs including the gully systems and their sedimentation areas.

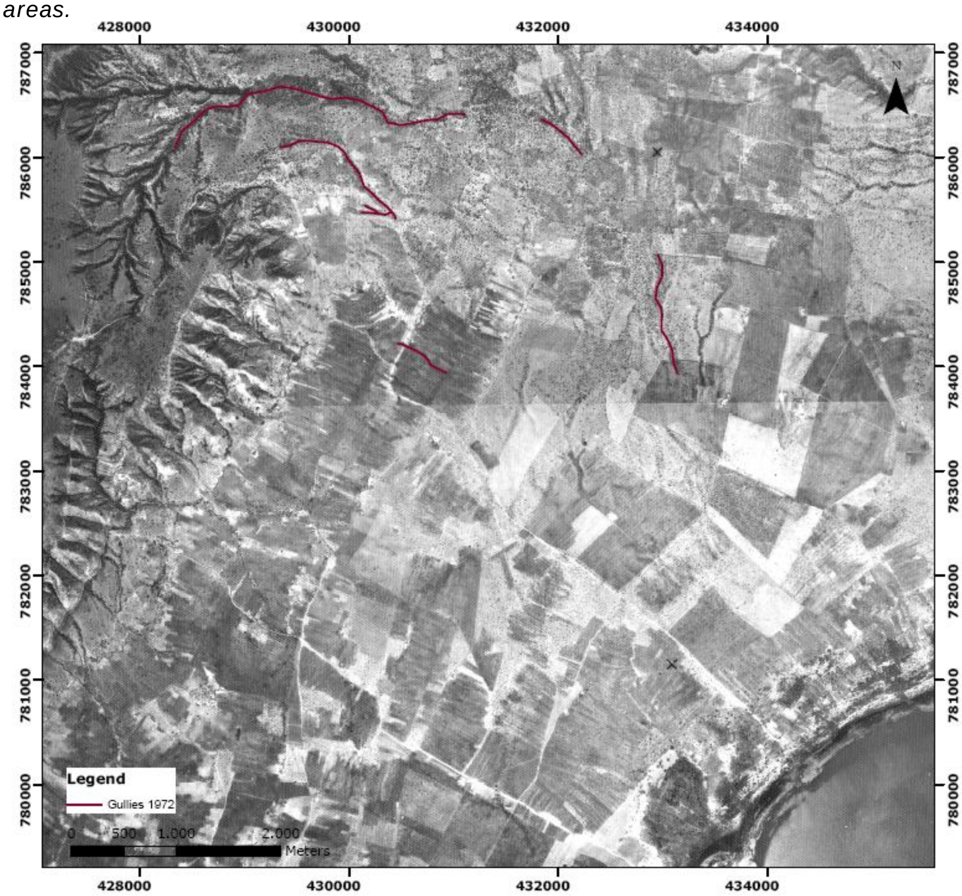

Fig. 4.2.6. The geo-referenced aerial photographs including the gullies that were there in 1972.

	Length in 1972	Percentage of length visible in 1972	V_0	V	$V-V_0$	Bd	V*Bd (t)	T	C	R_L
A	360	7.4	39214	527749	488536	0.724	353537			
B	1340	73.3	77894	106261	28367	0.829	23517			
C	0		0	151795	151795	0.751	114015			
D	0		0	3773	3773	0.751	2834			
E	0		0	4648	4648	0.751	3491			
F	0		0	38650	38650	0.751	29030			
G	0		0	49336	49336	0.751	37057			
H	0		0	8960	8960	0.742	6651			
I	0		0	20884	20884	0.787	16443			
J	569	54.3	28739	52881	24143	0.751	18134			
Gully system 1			**146000**	**965000**	**819000**		**605000**	**40**	**769**	**19.7**
Without gully I							**588000**			**19.1**
K	4853	37.9	656668	1734696	1078028	0.886	955313			
L	0		0	43793	43793	0.969	42436			
Gully system 2			**657000**	**1778000**	**1122000**		**998000**	**40**	**1913**	**13.0**

$$R_S = \frac{(V - V_0)Bd}{TC}$$

R_s is the area-specific short-term gully erosion rate (t ha^{-1}y^{-1})
V is volume of the gully (m^3)
V_0 is the initial gully volume at the beginning of the considered time span (m^3) (=V/100 * percentage of visible length)
Bd is the average dry bulk density of the soils occurring in the contributing area (t m^{-3})
T is the time span considered (years)
C is the watershed area (ha)

Table. 4.2.1. Length and volume per gully in 1972 and results of the calculation of the gully erosion rate over the last 40 years.

The activity of gully system 2 over the last 40 years is also analyzed by comparing the aerial photos with the most recent Landsat image of January 2011. Figure 4.2.7 and 4.2.8 show a zoomed-in image of the sedimentation area of the gully K and L in 1972 and 2011. Noticeable is the expansion of the land into Lake Awassa at this location, while the rest of the shoreline seems slightly withdrawn.

Fig. 4.2.7. Sedimentation area of gully of gully system in 1972 (source: Ethiopian Mapping Agency).

Fig. 4.2.7. Sedimentation area of gully system 2 in 2011 (source: Landsat 5 TM).

4.3 Land use classification

The results of the unsupervised land use classifications of the Landsat images are shown in the figures 4.3.1, 4.3.2 and 4.3.3. Based on observations in the field there are 4 classes used, distinguishing a high vegetation density from a low vegetation density. Class one contains a high vegetation density that consists of bushes and trees. The second class contains a medium vegetation density consisting of small bushes and high grasses. Class 3 are grasses and class 4 is bare soil.

Observations in the field show that dense vegetation can mainly be find up in the mountains. Further downhill on the gentle slopes the vegetation consists of small bushes and high grasses. The plain area is mainly used for agriculture containing crops like maize, aloe vera and enset. Besides the agriculture there are two areas in the northeast containing grass that are used for the cattle to graze. These grass fields come forward in the classified image of 2011 as well as the variation in vegetation density in the mountains in the west. The darker green areas around the grass fields are the fields with aloe vera. The plain area consists mainly of bare soil with some lanes of trees and bushes. The total area in hectares per class are listed in table 4.3.1. In 1994 the plain area is mainly bare soil as well, but there are no lanes of trees and bushes. In the northeast and southeast there are several areas containing grass with a higher vegetated field in the northeast corner of the study area. In the mountains in the west the vegetation makes a transition down slope from a high density to a lower density to low grasses at the foot. In 1986 this transition of vegetation in the mountains is visible as well. Different from 1994 and 2011 is that the plain area contains more dense vegetation and greater areas of vegetation.

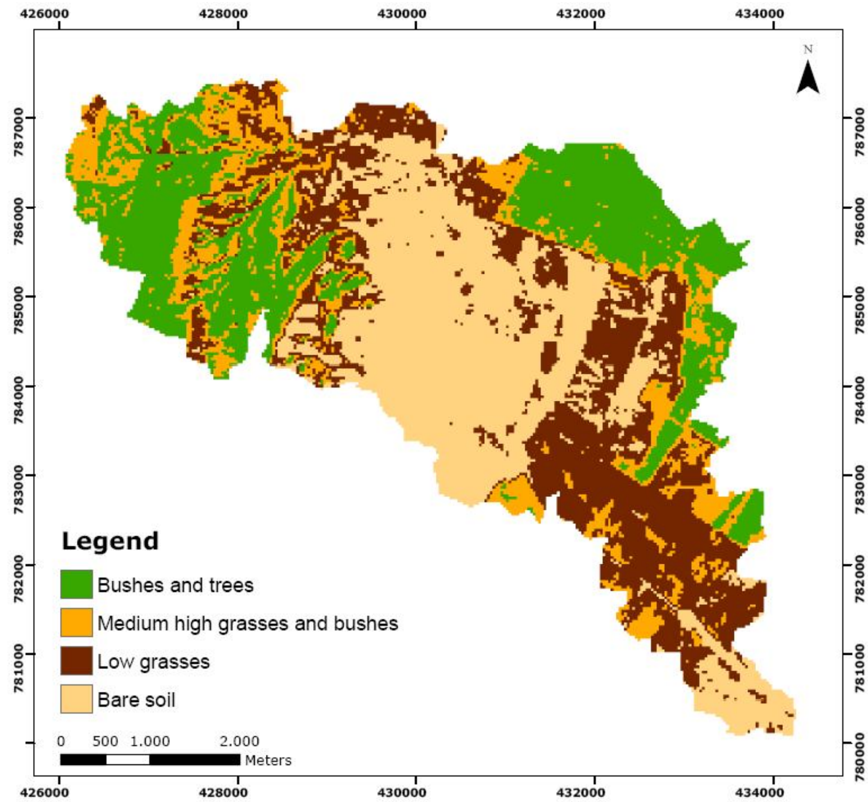

Fig. 4.3.1. Land use map of December 23, 1986 (source: Landsat 5 TM).

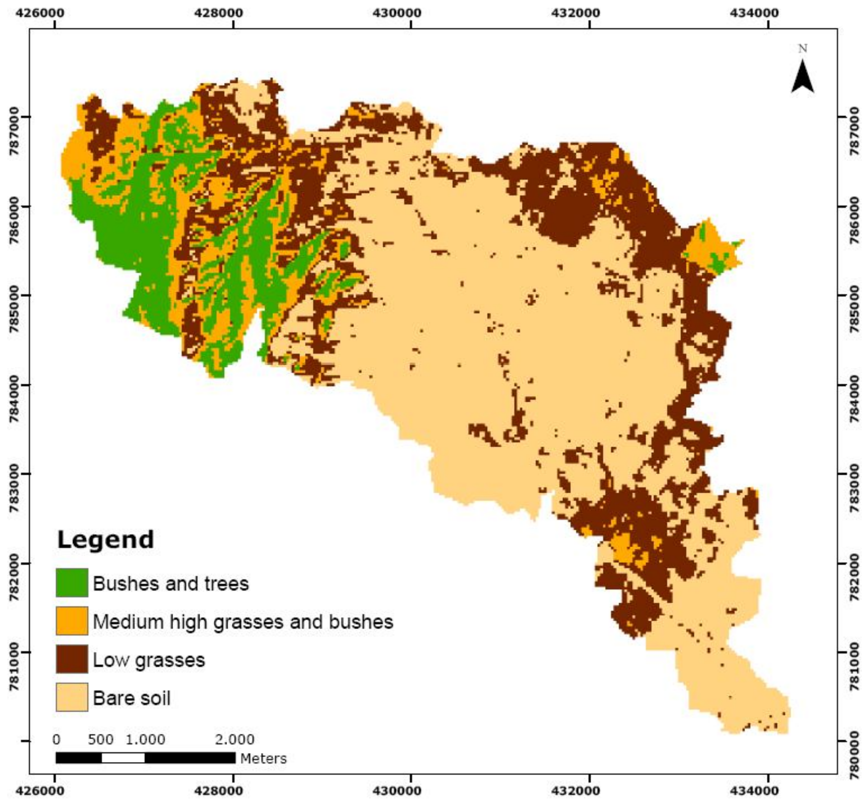

Fig 4.3.2. Land use map of December 13, 1994 (source: Landsat 5 TM).

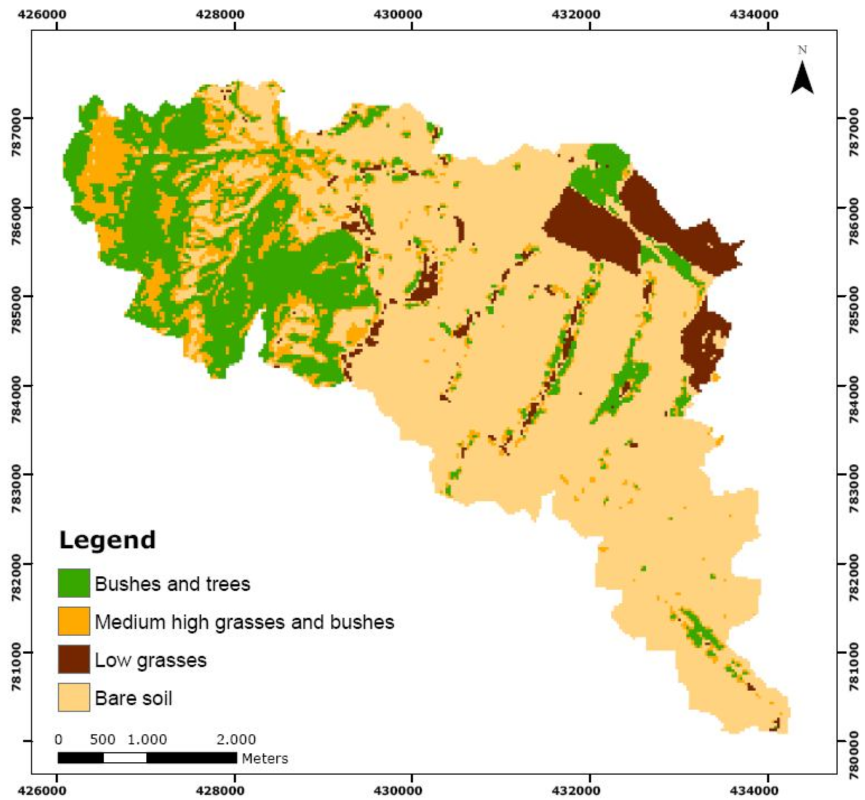

Fig. 4.3.3. Land use map of January 10, 2011 (source: Landsat 5 TM).

Table 4.3.1 shows for all the image the area in hectares per class. This table shows that the area of bare soil increased over time from 867 ha to 1639 ha. The area with low grasses decreases from 738 ha to 195 ha. In contrary, class 2 shows a decrease in area between 1986 to 1994 and the area increases again between 1994 and 2011. The area with bushes and trees is greatest in 1986 covering 646 ha while by 1994 the area is more than halved. In the period between 1994 and 2011 the area is doubled to 544 ha.

Class	**1986**	**1994**	**2011**
1) Bushes and trees	646	272	544
2) Medium high grasses and bushes	430	271	303
3) Low grasses	738	690	195
4) Bare soil	867	1447	1639

Table 4.3.1. Area per class per year in hectares according to the classified images.

5. Discussion

5.1 Gully dimension measurements

The results of the gully profile measurements carried out in the field can be defined accurate, in contrary to the results obtained with the stereo aerial photo analysis. The hook pattern in the digitized photos is the main cause of the failure in creating an accurate DTM. In the Automatic Terrain Extraction process the program recognizes the hooks and compares them in the photos, while the hooks are not in the exact same pixel in each photo. If this problem would have been solved, another problem could have arisen due to the low accuracy of the collected ground control points. The points have an average accuracy of 5 m in the x, y and z direction. This means that this is the highest resolution the DTM will have based on those points. Gullies with a depth around 1 and 2 m may still not be visible in the DTM. The visual evaluation of the aerial photos that is carried out is not accurate enough to give certain values of the gully volumes in 1972. Therefore the calculated area-specific short-term gully erosion rates are not comparable with other studies. However, the gully dimension measurements of the recent gully systems based on field measurements are accurate enough to do so. The study of Moges et al. (2008) shows similar gully dimension measurements and the calculated erosion rates are around the same values as calculated in this study. A difference between the gullies observed in their study and the gullies in this study is the variation in width. The gullies in this study have an average maximum width of about 25 m while in their study it is about 13 m. Besides that they also found pipe gullies in their study area which are not found in this study.

The results of the width-depth ratio measurements show in overall a decreasing value towards the gully end. In this case it means that the width increases and the depth decreases. Moges et al. (2008) found the same results in their study and they concluded that it is an indication for a decline in flow rate and potential sedimentation. During the field survey of this study there is observed that the sedimentation areas are at the end of the gullies where the width is greatest and the depth is smallest. This is indicated in the width-depth ratio graphs by a sudden increase in values towards the sedimentation areas. However, these sudden increases are not only visible towards the end of the gullies, but also further upstream for the gullies A, C, K and L. This indicates that not all the sediment is transported directly downstream, but is deposited temporarily in the gully until a new rain event transports it further downstream. A decline in flow rate indicates a decline in the slope angle. Assuming that this applies in the gullies, the variation of width-depth ratio values can be explained by a variations in the slope angle. When the slope angle increases, the flow rate increases which causes the gullies to develop more in depth than in width and results in a low width-depth ratio. This link cannot be proven with this study due to a lack in slope measurements. There was no possibility to carry them out in the field and there is no sufficient digital elevation model available to use that for the slope measurements.

5.2 Land use and changes and its effect on gully erosion

Field observations indicate that the plain area is mainly used for agriculture. However, when observing the classified image of January 2011 this area consists mainly of bare soil. This can be explained by the fact that the main crop in the area is maize. The maize grows in the rainy season and is harvested in the end of October and November. The three classified Landsat images are taken in December and January when the maize is already harvested and the fields contain nothing more than bare soil. These fields stay bare until the next rainy seasons, which means that these field are susceptible to erosion in the beginning of the rainy seasons when the maize did not grow back yet. From 1986 to 2011 the area of bare soil increases, but the vegetation density is higher in 2011 than in 1994. This can be explained by the fact that 1994 was a dry year compared to the other years. Even thought the density is lower, the plain area in 1994 contains more vegetation in the southeast than in 2011. This vegetation could be crops that were there as well in 1986. The results also indicate that the areas with trees and bushes and medium high grasses and bushes, decreases between 1986 and 1994 and increases again between 1994 and 2011 to about the same area as in 1986. This applies mainly to the mountain area and is due to closing of this area for cattle and replanting of vegetation in about the last 5 years. Besides the replanting in the mountains, the local people also planted vegetation in the gullies and gully heads. However, there are gully heads were no vegetation is planted while they are clearly active according to the recent wall collapses. Even in the gullies were vegetation is planted there are forms of activity visible like undercutting and wall collapses. The measures that are taken to prevent soil erosion by water, may decrease the runoff coming from the mountain area and may decrease the water erosion impact in the gullies. Besides that there are no observations made in the rainy season when the erosion actually takes place. However, there are observations made that indicate that the gullies are active according to the rules by Oostwoud et al. (2000). When gully erosion continuous in the following years, there is a great possibility that gully A will connect with gully L. This means that not only gully system 2 is connected to lake, but gully system 1 as well which will increase the deposition of sediments in Lake Awassa.

6. Conclusions and recommendations

The problem for the citizens of Awassa town in the Awassa watershed is the water level rise of lake Awassa, causing parts of the town to flood regularly. The aim of this study is to determine if the water level rise is due to siltation of the lake by gully erosion. After field survey of the sub catchment of the Awassa watershed and processing the aerial photos of 1972 and the Landsat imagery, the objectives and the goal of this research are achieved. In overall there can be concluded that the gullies are active and that gully erosion takes place, even though the measures that are taken to decrease it.

After gully dimension measurements in the field the volumes per gully system were calculated and their area-specific long-term gully erosion rate, assuming that the gullies developed exactly 40 years ago. Gully system 1 has a total volume in 2012 of 965000 m^3 and a gully erosion rate of 23.4 t $ha^{-1}y^{-1}$ when gully I is included. When gully I is not taken into account, because it is not connected to the other gullies, the gully erosion rate is 22.9 t $ha^{-1}y^{-1}$. For gully system 2 the total volume is 1778000 m^3 and its gully erosion rate is 20.7 t $ha^{-1}y^{-1}$. After calculations of the gully volumes in 1972 with the aerial photographs the gully erosion rate for gully system 1 is 19.7 t $ha^{-1}y^{-1}$ including gully I and 19.1 t $ha^{-1}y^{-1}$ excluding gully I. For gully system 2 the gully erosion rate is 13 t $ha^{-1}y^{-1}$. However, these rates are not accurate due to problems with digitizing the aerial photographs. When aerial photos can be digitized without errors, the recommendation is to collect more accurate and a greater amount of ground control points with for instance a Differential Global Positioning System (DGPS). The resolution of the DTM will be higher when using more accurate points and increases the visibility of the gullies and the accuracy of the gully dimension measurements.

Another objective was to link the land use changes and the gully erosion. There can be concluded that land use affects the water erosion in an area. In the study area there is a decrease in vegetation density in the mountains between 1986 and 1994. This causes the infiltration rate to decrease in that area which increases the runoff and thus the soil erosion by water. The maize crops are harvested at the beginning of the dry season, which leaves most of the plain area bare until the beginning of the rainy season. Bare soil is more vulnerable to erosion than vegetated areas, especially in the rainy season. In the last 40 years the bare soil increased from 867 ha in 1986 to 1639 ha in 2011 and means that more soil became vulnerable to gully erosion. To conclude with more certainty if there is a link between the land use changes and gully erosion, more research is necessary in the form of for instance determining the water balance of the area.

Eventually there can be concluded that gully system 1 has no connection with the lake and has its sedimentation area in the middle south of the study area. Gully system 2 is connected with the lake which is observed in the field. Besides that, when comparing the aerial photos of 1972 with the Landsat image of 2011, a land expansion into the lake is observed where gully K is connected with the lake. From these observations there can be concluded that there is a connection with Lake Awassa and the gullies and that sedimentation takes place in the lake due to gully erosion. According to the width-depth ratios, not all the sediment from the gullies K and L is deposited directly into the lake. Some sediment is deposited temporarily in the gully before it is transported further downstream during another rain event. There can be assumed that siltation of the lake by gully erosion takes place. However, erosion rates and the specific sediment yield cannot be given due to problems with processing the aerial photos.

References

Abiye, T.A. (2008). Environmental resources and recent impacts in the Awassa collapsed caldera, Main Ethiopian Rift. Quaternary International 189, 152-162.

Ayenew, T. (1998). The hydrogeological system of the lake district basin, Central Main Ethiopian rift. Published PhD thesis, Free University of Amsterdam, The Netherlands, 259.

Ayenew, T. (2001). Numerical groundwater flow modeling of the Central Main Ethiopian rift lakes basin. SINET: Ethiopian Journal of Science 24 (2), 167–184.

Ayenew, T. (2004). Environmental implications of changes in the levels of lakes in the Ethiopian Rift since 1970. Regional Environ. Change 4, 192–204.

Ayenew, T., Demellie, M., in press (2004). Bathymetric survey and estimation of the water balance of lake Ardibo, Northen Ethiopia. SINET: Ethiopian Journal of Science.

Ayenew, T., Gebreegziabher, Y. (2006). Application of a spreadsheet hydrological model for computing the long-term water balance of Lake Awassa, Ethiopia. Hydrological Sci. 51(3), 418-431.

Ayenew, T. (2007). Water management problems in the Ethiopian rift: challenges for development. J. Afr. Earth Sci. 48, 222–36.

Borgel, H., Arend, B., Jacobi, C., Kanyarukiga, S., Kullaya, S., Kullaya, A., Lemaga, B., Mogoeka, S., Wolfgang, P. (1980). Production, Marketing and Consumption of Potatoes in the Ethiopian Highlands (Holetta, Awassa, Alemaya). Centre for Advanced Training in Agricultural Development, Institute of Socio-Economics of Agricultural Development, Technical University of Berlin.

Brice, J.B. (1966). Erosion and deposition in the loess-mantled Great Plains, Medecine Creek drainage basin, Nebraska. U.S. Geological Survey Professional Paper 352H, 235– 339.

Chernet, T. (1982). Hydrology of the Lakes Region, Ethiopia (Lakes Ziway, Langano, Abiyata, Shalla and Awassa). Ethiopian Institute of Geological Survey. Addis Ababa, 97.

CSA (Central Statistics Authority), (1996). The 1994 Population and Housing Census of Ethiopia Results for Southern Nations, Nationalities and Peoples' Region. Central Statistics Authority, Addis Ababa.

Degefu, W. (1987). Some aspects of meteorological drought in Ethiopia. In: Glantz MH, editor. Drought and hunger in Africa: denying famine a future. Cambridge: Cambridge University Press, 23– 36.

Dessie, G. (2007). Forest Decline in South Central Ethiopia, Extent, history and process. PhD Thesis, Stockholm University, Sweden.

Dessie, G., Kleman, J. (2007a). Pattern and Magnitude of Deforestation in the South Central Rift Valley Region of Ethiopia. Mountain research and development 27(2), 162-168.

Dessie, G., Kinlund, P. (2007b). Khat Expansion and Forest Decline in Wondo Genet, Ethiopia. Geografiska Annaler (submitted).

ECX (Ethiopia Commodity Exchange), (2012). http://www.ecx.com.et/commodities.aspx; accessed on 8 July 2012.

EFAP (Ethiopian Forestry Action Program), (1994). Ethiopian Forestry Action Program, Vol. 2. The Challenge for Development. Ministry of Natural Resources Development and Environmental Protection, Addis Ababa.

FAO (Food and Agriculture Organization), (1984). Agroclimatological Data for Africa. Food and Agriculture Organization of the United Nations, Rome, Italy.

FAO, (2000). The Challenges of Sustainable Forestry Development in Africa. Yaoundé, Cameroon: FAO. Also available at: http://www.fao.org/docrep/meeting/x3976e.htm; accessed on 9 January 2007.

Foster, G.R. (1986). Understanding ephemeral gully erosion. Soil Conservation, vol. 2. National Academy of Science Press, Washington, DC, 90– 125.

Gamachu D. (1977). Aspects of climate and water budget in Ethiopia. Addis Ababa: Addis Ababa University Press.

Grissinger, E. (1996a). Rill and gullies erosion. In: Agassi, M. (Ed.), Soil Erosion, Conservation, and Rehabilitation. Marcel Dekker, New York, 153– 167.

Grissinger, E. (1996b). Reclamation of gullies and channel erosion. In: Agassi, M. (Ed.), Soil Erosion, Conservation, and Rehabilitation. Marcel Dekker, New York, 301– 313.

Hauge, C. (1977). Soil erosion definitions. California Geology 30, 202– 203.

Hurni, H. (1987). Erosion–productivity– conservation systems in Ethiopia. Pages 2–20 *in* Proceedings of the fourth international conference on soil conservation. Maracy, Venezuela. Imeson, A.C., Kwaad, F.J.P.M. (1980). Gully types and gully prediction. KNAG Geografisch Tijdschrift XIV 5, 430–441.

Leopold, L.B., Wolman, M.G., Miller, J.P. (1964). Fluvial processes in geomorphology. Freeman, San Fransisco.

Makin, M.J., Kingham, T.J., Waddams, A.E., Birchall, C.J., Eavis, B.W. (1976). Prospects for irrigation development around lake Ziway, Ethiopia. Land Res. Study. Division, Ministry of Overseas development 26, Tolworth, UK, 270.

Medhin, G., Giorgis, W., Gebre, E., Bedane, K., Kassa, B. (2001). Country Profile on Potato Production and Utilization: Ethiopia. Ethiopian Agricultural Research Organization (EARO), Holetta Agricultural Research Centre, National Potato Research Program.

Moges, A., Holden, N.M. (2008). Estimating the rate and consequences of gully development, a case study of Umbulo catchment in Southern Ethiopia. Land Degradation and Development 19, 574-586.

Nyssen, J. (2001). Erosion processes and soil conservation in a tropical mountain catchment under threat of anthropogenic desertification—a case study from Northern Ethiopia. Unpubl. PhD thesis, Dept. Geography–Geology, K.U. Leuven, Belgium.

Nyssen, J., Veyret Picot, M., Poesen, J., Moeyersons, J., Mitiku, H., Deckers, J., Govers, G. (2004a). The effectiveness of loose rock check dams for gully control in Tigray, northern Ethiopia. Soil Use and Management 20 (1), 55–64.

Nyssen, J., Poesen, J., Moeyersons, J., Deckers, J., Mitiku, H. (2004b). Erosion et conservation des sols en montagne sahe´lienne, le cas de l'Ethiopie du Nord. Se´cheresse 15 (1), 33– 39.

Nyssen, J., Poesen, J., Veyret-Picot, M., Moeyersons, J., Haile, M., Deckers, J., Dewit, J., Naudts, J., Teka, K., Govers, G. (2006). Assessment of gully erosion rates through interviews and measurements: a case study from northern Ethiopia. Earth Surf. Process. and Landforms 31, 167-185.

Oostwoud, W.D.J., Poesen, J., Vandekerckhove, L., Ghesquiere, M. (2000). Spatial distribution of gully head activity and sediment supply along an ephemeral channel in a Mediterranean environment. Catena 39,147–167.

Poesen, J. (1993). Gully typology and gully control measures in the European loess belt. In: Wicherek, S. (Ed.), Farm Land Erosion in Temperate Plains Environment and Hills. Elsevier, Amsterdam, 221– 239.

Poesen, J., Nachtergaele, J., Verstraeten, G., Valentin, C. (2003). Gully erosion and environmental change: importance and research needs. Catena 50, 91-133.

Reusing, M. (1998). Monitoring of Natural High Forest Resources in Ethiopia. Addis Ababa, Ethiopia: Ministry of Agriculture.

Russ, G.W. (1944). Reports on Ethiopian Forests. Compiled in 1979 by Wolde-Michael Kelecha. Addis Ababa, Ethiopia: Ministry of Agriculture.

Sheikh, B.A., Soomro, G.H. (2006). Desertification: causes, consequences and remedies. Pak J Agri Agril Engg Vet Sci 22, 44–51.

Soil Science Society of America, (2001). Glossary of Soil Science Terms. Soil Science Society of America, Madison, WI, http://www.soils.org/sssagloss/.

Taddese, G. (2001). Land degradation: A challenge to Ethiopia. Environ. Management Vol 27, 6, 815-824.

Telford, R.J., Lamb, H.F., Mohammed, M.U. (1999). Diatom-derived palaeoconductivity estimates for Lake Awassa, Ethiopia; evidence for pulsed inflows of saline groundwater. J. Paleolimnol. 21, 409–421.

Telford, R.J. (2000). Diatom stratigraphies of lakes Awassa and Tilo, Ethiopia: Holocene records of groundwater variability and climate change. PhD Thesis, University of Wales, UK.

Tesfahunegn, G.B., Vlek, P.L.G., Tamene, L. (2012). Management strategies for reducing soil degradation through modeling in a GIS environment in northern Ethiopia catchment. Nutr. Cycl. Agroecosyst. 92, 255-272.

Tessema, Z. (1998). Hydrochemical and water balance approach in the study of high water level rise of lake Beseka. M.Sc thesis, The University of Birmingham, 90.

Tulu, T. (2011). Soil and water conservation for sustainable agriculture. Mega Publishing and Distribution P.L.C., Addis Ababa, Ethiopia, 2011.

USDA (United States Department of Agriculture), (2008). Ethiopia 2008 crop assessment travel report. Available at: http://www.pecad.fas.usda.gov/highlights/2008/11/eth_25nov2008/; accessed on 8 July 2012.

Valentin, C., Poesen, J., Li, Y. (2005). Gully erosion: Impacts, factors and control. Catena 63, 132-153.

WBISPP (Woody Biomass Inventory and Strategic Planning Project), (2004). Forest Resources of Ethiopia. Addis Ababa, Ethiopia: Ministry of Agriculture.

Wood, R.B., Talling, J.F. (1988). Chemical and algal relationship in a salinity series of Ethiopian inland waters. Hydrobiologia 158, 29–67.

WWDSE (Water Works Design and Supervision Enterprise) (2001). The study of Lake Awassa level rise. Southern Nations Nationalities and Peoples Regional State. Water, Mines and Energy Resources Development Bureau. Unpublished report of the Water Works Design and Supervision Enterprise (main report volume II), Addis Ababa, Ethiopia.

Appendices

Appendix A Sub catchments per gully systems

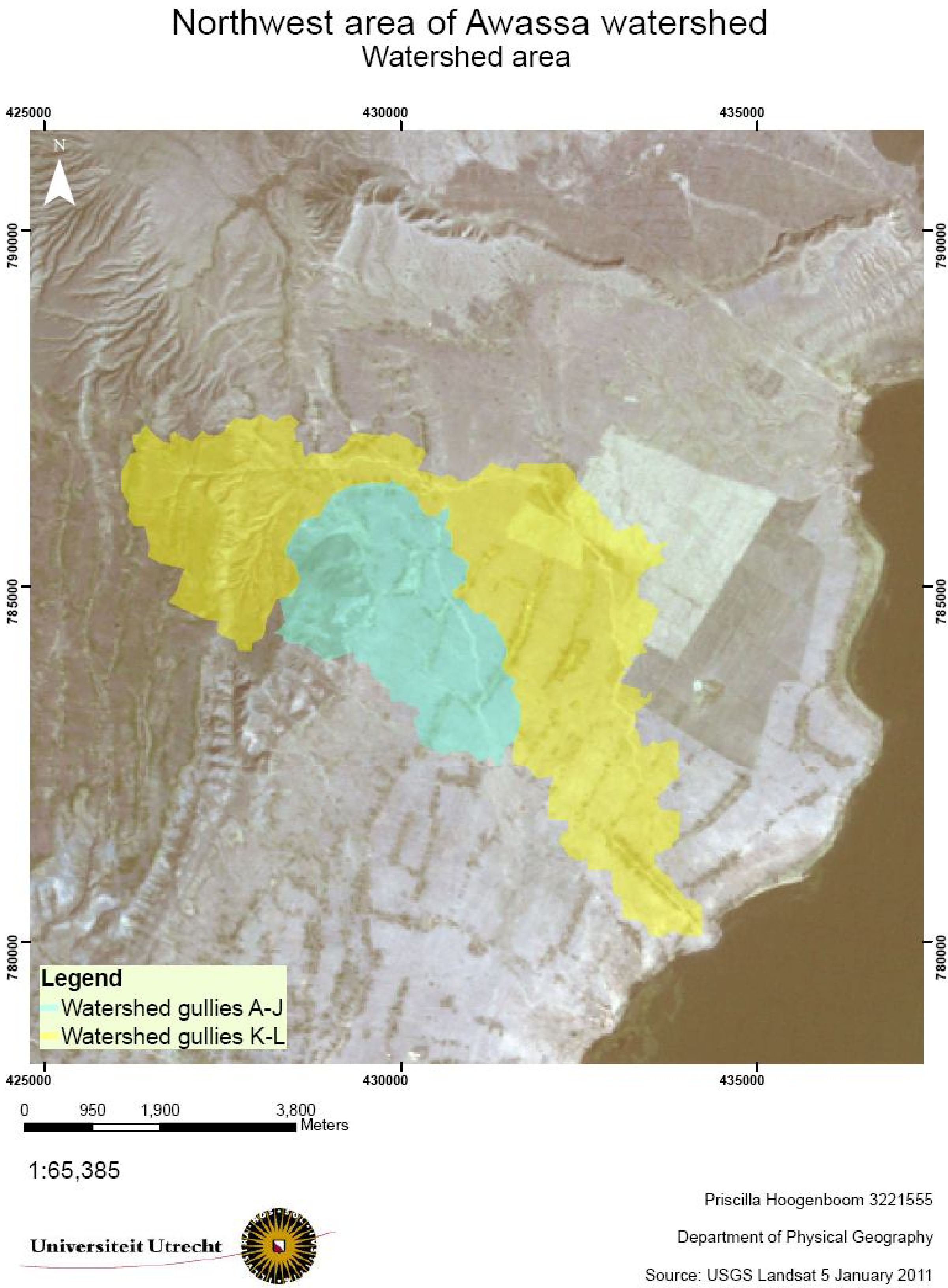

Appendix B Overview of the collected field data

Points of gully profiles

Gully	GPS point	Lat	Long	Date&time	z (m)	EPE (m)	depth (m)	bottom (m)	area (m2)	width/depth ratio	soiltype	photos
A1	36	431107	783266	16-oct-12 12:10	1723	5.4	1.5	54.1	81.2	36.1	sandy loam	660-662
A2	37	431086	783338	16-oct-12 12:24	1724	4.0	2.1	49.0	102.9	23.3	sandy loam	663-665
A3	38	431162	783553	16-oct-12 12:31	1720	4.3	1.3	28.0	36.4	21.5	sandy loam	665-667
A4	41	431053	783998	16-oct-12 12:42	1728	4.0	1.8	47.0	84.6	26.1	sandy loam	671
A5	42	430839	784562	16-oct-12 12:57	1742	3.9	1.8	63.0	113.4	35.0	sandy loam	672-675
A6	44	430718	784789	16-oct-12 13:07	1746	4.3	6.8	29.0	197.2	4.3	sandy loam/volcanic ash	676-682
A7	45	430582	785047	16-oct-12 13:14	1751	4.4	9.0	23.3	209.7	2.6	sandy loam/volcanic ash/?	683-689
A8	46	430470	785436	16-oct-12 13:29	1763	4.2	6.0	24.0	144.0	4.0	sandy loam/volcanic ash/?	
A9	48	430324	785482	16-oct-12 13:37	1763	3.9	7.0	11.6	81.2	1.7		690-692
A10	49	430065	785534	16-oct-12 13:46	1775	4.0	4.4	18.0	79.2	4.1	sandy loam/volcanic ash/?	693-699
A11	50	429890	785589	16-oct-12 14:13	1785	3.9	4.4	18.0	79.2	4.1		700-701
A12	51	429535	785658	16-oct-12 14:21	1796	3.8	10.1	11.5	116.2	1.1		702-704

Gully	GPS point	Lat	Long	Date&time	z (m)	EPE (m)	depth (m)	bottom (m)	area (m2)	width/depth ratio	soiltype	photos
B1	55	430314	785589	16-oct-12 14:43	1769	4.1	8.5	10.5	89.3	1.2		717-720
B2	57	430079	785915	16-oct-12 14:59	1781	4.6	5.0	16.0	80.0	3.2	sandy loam/volcanic ash/sandy loam	743
B3	59	429986	786040	16-oct-12 15:04	1786	5.0	3.0	7.0	21.0	2.3	mainly sandy loam	
B4	60	429896	786159	16-oct-12 15:08	1790	3.9	2.3	16.5	38.0	7.2	mainly sandy loam	749-751
B5	61	429780	786173	16-oct-12 15:12	1793	4.0	2.5	6.0	15.0	2.4	mainly sandy loam	
B6	62	429682	786163	16-oct-12 15:14	1797	4.0	2.1	8.6	18.1	4.1	mainly sandy loam	752-756
B7	64	429412	786147	16-oct-12 15:21	1812	4.2	6.0	12.0	72.0	2.0	mainly sandy loam	759-762
B8	66	429306	786119	16-oct-12 15:29	1814	5.1	9.0	7.0	63.0	0.8		771-773

Gully	GPS point	Lat	Long	Date&time	z (m)	EPE (m)	depth (m)	bottom (m)	area (m2)	width/depth ratio	soiltype	photos
C1	155	431025	783324	17-oct-12 10:31	1713	4.3	1.6	35.4	56.6	22.1	sandy loam	
C2	156	430754	783508	17-oct-12 10:40	1727	3.9	2.0	17.0	34.0	8.5	sandy loam	775-779
C3	157	430596	783564	17-oct-12 10:45	1721	4.5	1.8	65.0	117.0	36.1	sandy loam, start volcanic ash	780-783
C4	158	430441	783744	17-oct-12 10:54	1736	4.3	9.0	13.5	121.5	1.5	sandy loam/volcanic ash/sandy loam	784-785
C5	160	430315	783819	17-oct-12 11:01	1737	5.7	8.0	4.0	32.0	0.5	sandy loam/volcanic ash/sandy loam	786-788
C6	163	430232	783867	17-oct-12 11:15	1743	7.5	7.5	3.8	28.5	0.5	sandy loam/volcanic ash/sandy loam	793-794

C7	165	429993	783940	17-oct-12 11:23	1753	3.9	7.0	9.0	63.0	1.3	sandy loam/volcanic ash/sandy loam	798
C8	166	429701	784061	17-oct-12 11:34	1765	4.3	6.0	3.2	19.2	0.5	sandy loam/volcanic ash/sandy loam	
C9	167	429583	784108	17-oct-12 11:40	1769	4.9	8.5	2.1	17.9	0.2	sandy loam/volcanic ash/sandy loam	800

Gully	GPS point	Lat	Long	Date&time	z (m)	EPE (m)	depth (m)	bottom (m)	area (m2)	width/depth ratio	soiltype	photos
D1	162	430322	783827	17-oct-12 11:06	1735	3.3	6.5	4.5	29.3	0.7	sandy loam	

Gully	GPS point	Lat	Long	Date&time	z (m)	EPE (m)	depth (m)	bottom (m)	area (m2)	width/depth ratio	soiltype	photos
E1	169	430180	783923	17-oct-12 12:07	1746	4.6	6.5	2.6	16.9	0.4		

Gully	GPS point	Lat	Long	Date&time	z (m)	EPE (m)	depth (m)	bottom (m)	area (m2)	width/depth ratio	soiltype	photos
F1	171	430357	783955	17-oct-12 13:21	1743	3.7	7.0	5.5	38.5	0.8	sandy loam/volcanic ash/sandy loam	801-802
F2	172	430262	784136	17-oct-12 13:27	1745	4.7	6.0	13.0	78.0	2.2	sandy loam/volcanic ash/sandy loam	804
F3	174	430204	784198	17-oct-12 13:35	1750	3.9	6.0	8.0	48.0	1.3	sandy loam/volcanic ash/sandy loam	808

Gully	GPS point	Lat	Long	Date&time	z (m)	EPE (m)	depth (m)	bottom (m)	area (m2)	width/depth ratio	soiltype	photos
G1	175	430219	784271	17-oct-12 13:40	1752	3.9	3.0	17.0	51.0	5.7	sandy loam/volcanic ash/sandy loam	809-810
G2	176	430097	784358	17-oct-12 13:43	1756	3.8	4.0	8.5	34.0	2.1	mainly sandy loam	811-812
G3	177	429856	784507	17-oct-12 13:49	1764	3.5	9.0	3.0	27.0	0.3	sandy loam/volcanic ash/sandy loam	
G4	179	429789	784749	17-oct-12 13:56	1774	3.0	5.5	10.3	56.7	1.9	mainly sandy loam	
G5	181	429707	784790	17-oct-12 14:02	1780	5.3	10.0	5.0	50.0	0.5	sandy loam/volcanic ash/sandy loam	817-818

Gully	GPS point	Lat	Long	Date&time	z (m)	EPE (m)	depth (m)	bottom (m)	area (m2)	width/depth ratio	soiltype	photos
H1	184	429751	784875	17-oct-12 14:18	1777	3.0	4.0	10.0	40.0	2.5	sandy loam/volcanic ash/sandy loam	828-829
											sandy loam/volcanic ash/sandy loam	

Gully	GPS point	Lat	Long	Date&time	z (m)	EPE (m)	depth (m)	bottom (m)	area (m2)	width/depth ratio	soiltype	photos
I1	187	430213	784981	17-oct-12 14:29	1761	3.8	7.0	8.4	58.8	1.2	sandy loam/volcanic ash/sandy loam	12okt foto's
I2	188	430270	784843	17-oct-12 14:35	1756	3.6	4.0	9.8	39.2	2.5	sandy loam/volcanic ash	830-832
I3	189	430405	784706	17-oct-12 14:38	1750	4.1	2.0	11.3	22.6	5.7	sandy loam	833-834
I4	190	430492	784624	17-oct-12 14:43	1750	3.6	1.0	12.0	12.0	12.0	sandy loam	835

Gully	GPS point	Lat	Long	Date&time	z (m)	EPE (m)	depth (m)	bottom (m)	area (m2)	width/depth ratio	soiltype	photos
J1	193	430327	784303	17-oct-12 14:58	1745	3.7	6.0	6.0	36.0	1.0	sandy loam/volcanic ash/sandy loam	837-838
J2	192	430419	784235	17-oct-12 14:55	1737	4.0	6.0	3.0	18.0	0.5	mainly sandy loam	836
J3	195	430549	784203	17-oct-12 15:11	1736	4.1	4.0	11.7	46.8	2.9	mainly sandy loam	842

J4	196	430779	784057	17-oct-12 15:16	1730	3.8	4.0	21.0	84.0	5.3	mainly sandy loam	843-845
J5	197	430896	783962	17-oct-12 15:20	1726	3.6	3.0	17.1	51.3	5.7	mainly sandy loam	846

Gully	**GPS point**	**Lat**	**Long**	**Date&time**	**z (m)**	**EPE (m)**	**depth (m)**	**bottom (m)**	**area (m2)**	**width/depth ratio**	**soiltype**	**photos**
K1	4	428289	786108	18-oct-12 11:20	1860	4.8	6.0	22.0	132.0	3.7	mainly sandy loam	
K2	5	428498	786356	18-oct-12 11:28	1848	3.1	8.0	16.6	132.8	2.1	mainly sandy loam	854-857
K3	6	428630	786438	18-oct-12 11:34	1842	3.8	6.0	13.7	82.2	2.3	mainly sandy loam	858-859
K4	7	428807	786539	18-oct-12 11:41	1835	4.1	9.0	15.5	139.5	1.7	7 soil layers	860-864
K5	9	429318	786804	18-oct-12 11:58	1807	4.0	11.0	36.5	401.5	3.3	7 soil layers	872-876
K6	10	429896	786687	18-oct-12 12:10	1794	3.8	8.0	33.5	268.0	4.2	mainly sandy loam	877-879
K7	11	430224	786589	18-oct-12 12:20	1786	3.8	5.0	44.0	220.0	8.8	mainly sandy loam	880-887
K8	12	430563	786391	18-oct-12 12:30	1777	4.1	6.0	76.5	459.0	12.8	mainly sandy loam	888-892
K9	13	431117	786518	18-oct-12 12:43	1765	4.1	2.5	39.0	97.5	15.6	mainly sandy loam	893-894
K10	14	431695	786546	18-oct-12 13:22	1754	3.6	2.0	14.0	28.0	7.0	mainly sandy loam	
K11	16	432072	786297	18-oct-12 13:32	1742	3.8	1.2	14.0	16.8	11.7	mainly sandy loam	895-898
K12	19	432407	785934	18-oct-12 13:44	1736	3.5	2.5	66.2	165.5	26.5	mainly sandy loam	907-912
K13	20	432677	785571	18-oct-12 13:54	1731	3.7	2.3	35.2	81.0	15.3	mainly sandy loam	
K14	23	432968	785035	18-oct-12 14:09	1726	3.8	2.2	55.0	121.0	25.0	mainly sandy loam	924-925
K15	26	433105	783741	18-oct-12 14:35	1714	4.4	5.0	46.0	230.0	9.2	mainly sandy loam	
K16	27	433214	783199	18-oct-12 14:49	1712	4.5	3.5	37.0	129.5	10.6	mainly sandy loam	948-954
K17	28	433243	782791	18-oct-12 14:57	1706	4.6	2.0	42.3	84.6	21.2	mainly sandy loam	
K18	30	433352	782307	18-oct-12 15:05	1704	4.0	1.9	24.5	46.6	12.9	mainly sandy loam	
K19	31	433455	782184	18-oct-12 15:09	1700	3.6	3.0	20.2	60.6	6.7	mainly sandy loam	955-961
K20	32	433498	781972	18-oct-12 15:14	1696	4.4	2.2	8.2	18.0	3.7	mainly sandy loam	962-963
K21	33	433539	781739	18-oct-12 15:18	1696	4.4	1.5	8.0	12.0	5.3	mainly sandy loam	964-965
K22	34	433540	781380	18-oct-12 15:23	1694	4.5	1.7	13.3	22.6	7.8	mainly sandy loam	
K23	35	433521	781042	18-oct-12 15:28	1692	4.0	2.0	13.0	26.0	6.5	mainly sandy loam	
K24	44	433507	780931	24-oct-12 11:13	1686	4.1	1.7	21.2	36.0	12.5	mainly sandy loam	972
K25	45	433664	780797	24-oct-12 11:18	1687	3.9	2.1	15.7	33.0	7.5	mainly sandy loam	972-973
K26	46	433873	780581	24-oct-12 11:23	1689	3.4	1.9	15.0	28.5	7.9	mainly sandy loam	974-975
K27	47	434038	780382	24-oct-12 11:28	1685	3.7	1.3	11.2	14.6	8.6	mainly sandy loam	976-977

Gully	**GPS point**	**Lat**	**Long**	**Date&time**	**z (m)**	**EPE (m)**	**depth (m)**	**bottom (m)**	**area (m2)**	**width/depth ratio**	**soiltype**	**photos**
L1	52	433450	780982	24-oct-12 11:51	1689	3.9	2.0	23.7	47.4	11.9	mainly sandy loam	
L2	53	433328	781098	24-oct-12 11:55	1689	4.0	2.0	17.0	34.0	8.5	mainly sandy loam	2

L3	54	433121	781305	24-oct-12 11:59	1690	4.6	1.5	11.2	16.8	7.5	mainly sandy loam		
L4	55	433021	781412	24-oct-12 12:02	1689	4.2	2.0	14.1	28.2	7.1	mainly sandy loam		
L5	56	432891	781508	24-oct-12 12:05	1689	4.3	1.9	10.8	20.5	5.7	mainly sandy loam		3
L6	58	432754	781617	24-oct-12 12:10	1693	4.4	1.2	12.4	14.9	10.3	mainly sandy loam		
L7	59	432648	781706	24-oct-12 12:14	1693	4.6	1.8	9.8	17.6	5.4	mainly sandy loam		
L8	60	432490	781848	24-oct-12 12:17	1696	4.5	1.9	14.4	27.4	7.6	mainly sandy loam	004-005	
L9	61	432377	781938	24-oct-12 12:20	1697	3.9	1.2	17.0	20.4	14.2	mainly sandy loam		6
L10	62	432279	782008	24-oct-12 12:24	1697	4.2	1.3	15.0	19.5	11.5	mainly sandy loam		
L11	63	432157	782097	24-oct-12 12:28	1699	4.0	0.6	16.8	10.1	28.0	mainly sandy loam	007-008	

Rest of the collected points

GPS point	Gully	Lat	Long	Date&time	z (m)	Description	EPE (m)	Photos
40	A	431063	783903	16-oct-12 12:40	1726	Splitsing met niet actieve gully	4.6	667-670
43	A	430794	784688	16-oct-12 13:02	1744	Start volcanic ash layer	4.5	
47	A	430390	785500	16-oct-12 13:33	1763	Splitsing	4.9	
52	A	429511	785715	16-oct-12 14:25	1803	Gully recover	3.5	707
53	A	429453	785805	16-oct-12 14:27	1808	Gully beginning	3.8	708-709
54	A	429316	785966	16-oct-12 14:31	1829	Gully start, rest vegetated	4.1	713-715
56	B	430090	785792	16-oct-12 14:52	1778	Splitsing	4.2	728-734
58	B	430015	786022	16-oct-12 15:03	1786		4.8	742-748
63	B	429521	786187	16-oct-12 15:18	1808	Gully recovering from B6	4.6	757-758
65	B	429383	786120	16-oct-12 15:24	1813	3m volcanic ash, 3m soil rest gully recovering	4.1	763-766
66	B	429306	786119	16-oct-12 15:29	1814	vegetated	5.1	767-767
159	C	430358	783791	17-oct-12 10:57	1740	Splitsing	4.6	
161	C/D	430288	783834	17-oct-12 11:02	1729	Splitsing	6.2	789-792
164	C	430034	783922	17-oct-12 11:20	1746	Gully becomes wider	4.8	795-797
166	C	429701	784061	17-oct-12 11:34	1765	Splitsing	4.3	
168	C	429773	784047	17-oct-12 11:46	1760	Beginning deeper part, about 2m deeper	4.0	
170	E	430108	783979	17-oct-12 12:10	1750	Begin gully E	3.9	
172	F	430262	784136	17-oct-12 13:27	1745	Splitsing	4.7	804
173	F	430147	784240	17-oct-12 13:32	1746	Beginning gully F	6.1	805-807
178	G	429815	784668	17-oct-12 13:54	1771	Diepe gully uitsnede	4.0	815-816
180	G	429770	784804	17-oct-12 13:59	1779	Splitsing	4.4	
182	G	429680	784785	17-oct-12 14:04	1782	Begin gully G X	8.0	
183	G	429617	784726	17-oct-12 14:09	1801	Real begin gully G	4.0	819-827

184	H	429751	784875	17-oct-12 14:18	1777	Vegetated from here	3.0	828-829
186	I	430177	785038	17-oct-12 14:28	1772	Begin gully, gully head I	3.9	
190	I	430492	784624	17-oct-12 14:43	1750	End gully I	3.6	835
191	J	430473	784230	17-oct-12 14:52	1741	Vegetated gully J	3.9	
194	J	430224	784379	17-oct-12 15:01	1748	Begin gully J	3.6	839-840
198	J/A	431049	783908	17-oct-12 15:24	1724	Connection gully J with A	3.6	847
1	A	431411	782704	18-oct-12 10:29	1707	End gully A (sand loam)	4.5	
3	K	428289	786089	18-oct-12 11:16	1863	Start gully measuring	4.0	848-853
8	K	429021	786588	18-oct-12 11:47	1824	Splitsing	4.3	865-871
24	K	432963	784591	18-oct-12 14:18	1725	Splitsing	4.2	926-944
25	K	433069	784125	18-oct-12 14:30	1719	Gully becomes smaller	4.5	947
36	K	433471	780966	18-oct-12 15:30	1694	Splitsing	3.8	966-971
43	K	433482	780962	24-oct-12 11:11	1687	Splitsing	4.8	
49	K	434164	780235	24-oct-12 11:33	1687	Gully wider to the lake	3.9	978-980
50	K	434195	780208	24-oct-12 11:35	1686	Deposition sediment, former shore at the end of tabak field	4.0	981-988
51	K	434493	780071	24-oct-12 11:41	1687	End deposition area	4.3	989-001
64	L	432108	782127	24-oct-12 12:30	1698	Begin gully L	4.2	009-010
76	A	429924	785582	24-oct-12 15:11	1784	Soil in gully A vanaf hier heuvelopwaarts zoals gully B	5.3	

Landuse

GPS point	Pointnr	Lat	Long	Date&time	z (m)	Land use	EPE (m)	Photos
36	1	431107	783266	16-oct-12 12:10	1723	N: maize Z: maize	5.4	
39	2	431079	783734	16-oct-12 12:36	1724	N: maize Z: maize W: maize	4.7	
54	3	429316	785966	16-oct-12 14:31	1829	NW: ensat field	4.1	716
60	4	429896	786159	16-oct-12 15:08	1790	N: maize Z: maize	3.8	749-751
66	5	429306	786119	16-oct-12 15:29	1814	W: Ensat	5.1	773
185	6	429914	784960	17-oct-12 14:24	1779	NW: ensat field (west of football, grass field)	4.2	
2	7	428740	786352	18-oct-12 10:57	1852	E: ensat W: maize	4.5	
13	8	431117	786518	18-oct-12 12:43	1765	E: maize	4.1	893-894
15	9	431908	786511	18-oct-12 13:27	1749	Qancha (Aloe)	3.7	
17	10	432189	786119	18-oct-12 13:38	1741	Aloe	3.8	899-903
18	11	432330	785986	18-oct-12 13:42	1741	N: grass	4.1	904-906
21	12	432811	785396	18-oct-12 14:00	1726	SW: maize E: Aloe	4.4	915-917
22	13	432911	785253	18-oct-12 14:05	1728	Aloe baricade	3.8	918-923

29	14	433271	782686	18-oct-12 15:00	1707	W&E: maize	3.7	955-956
38	15	431751	781478	24-oct-12 10:49	1700	N&S maize	4.5	
39	16	433498	779733	24-oct-12 10:54	1683	N&S maize, E near lake swampy	5.2	
41	17	432520	779305	24-oct-12 11:01	1691	N&S maize	3.2	
42	18	433436	780651	24-oct-12 11:06	1690	W&E maize	4.9	
49	19	434164	780235	24-oct-12 11:33	1687	N tabak	3.9	981-988
50	20	434195	780208	24-oct-12 11:35	1686	Bare soil	4.0	981-988
57	21	432789	781585	24-oct-12 12:09	1693	N&S maize	4.4	
62	22	432279	782008	24-oct-12 12:24	1697	N&S maize	4.2	
68	23	432110	786013	24-oct-12 13:42	1741	grassfield, N aloe vera + gully K	4.5	011-013
69	24	431335	785585	24-oct-12 13:46	1746	E ensat	5.1	
70	25	430863	784948	24-oct-12 13:49	1743	E&W ensat	5.2	
72	26	430125	785748	24-oct-12 14:14	1767	S maize	5.6	14-17
73	27	428624	786396	24-oct-12 14:45	1849	N ensat W hilly area, bushes	4.0	
75	28	429098	786111	24-oct-12 15:03	1847	W bushes on hills & few small trees	3.6	18-22

Appendix C Gully measurement locations

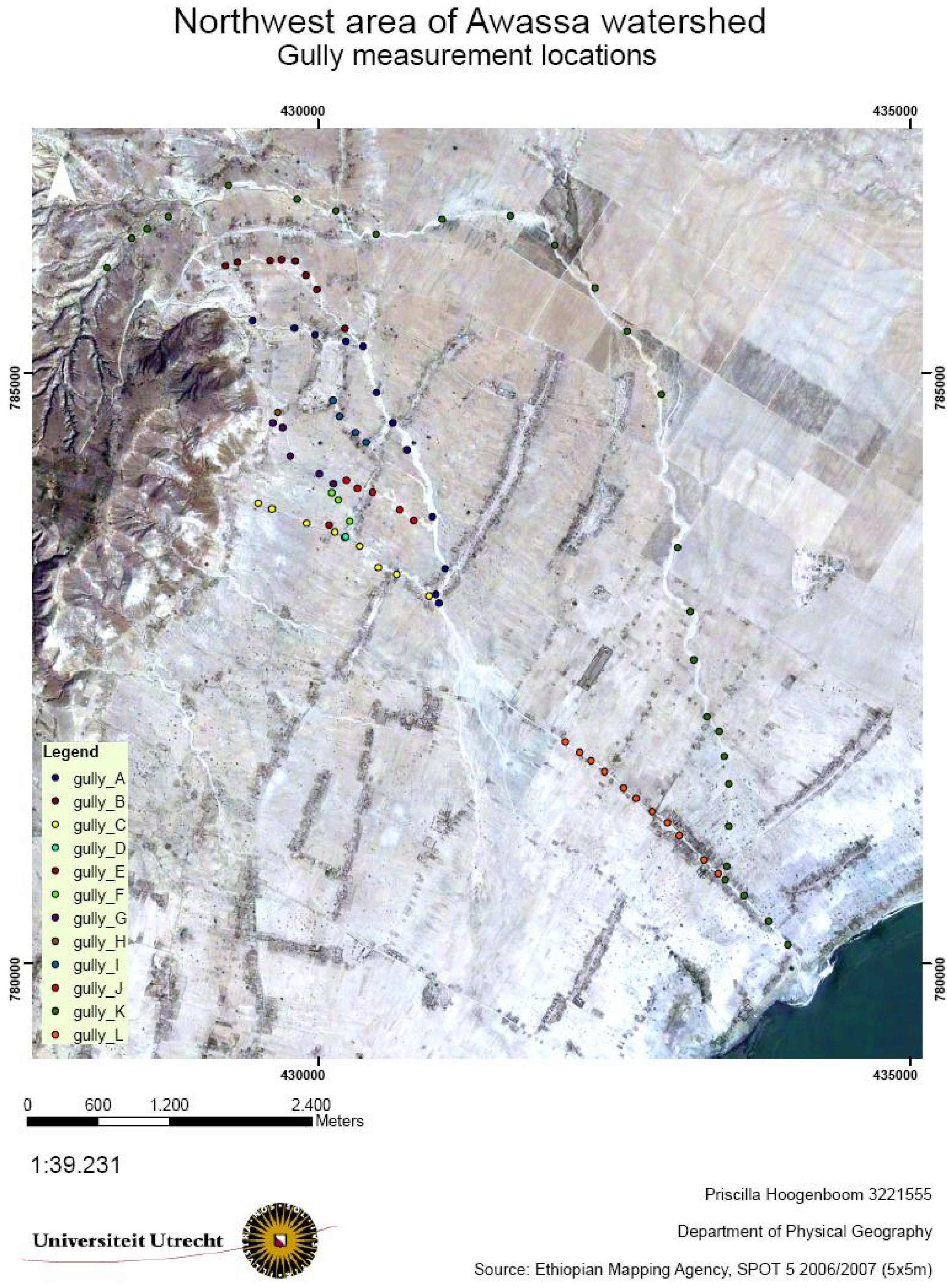

Appendix D Land use sample and soil sample locations